ANESTHESIOLOGY

Slick Potassium Channels Control Pain and Itch in Distinct Populations of Sensory and Spinal Neurons in Mice

Cathrin Flauaus, R.Ph., Patrick Engel, R.Ph., Fangyuan Zhou, M.S., Jonas Petersen, Ph.D., Peter Ruth, Ph.D., Robert Lukowski, Ph.D., Achim Schmidtko, M.D., Ph.D., Ruirui Lu, M.D., Ph.D.

Anesthesiology 2022; 136:802–22

EDITOR'S PERSPECTIVE

What We Already Know about This Topic

- The activity of sensory and dorsal horn neurons controls the sensations of pain and itch
- The recently identified potassium ion channel Slick is expressed on sensory and spinal neurons, but its functional roles are poorly understood

What This Article Tells Us That Is New

- Using male and female mouse models, it was observed that Slick reduces responses to noxious thermal and chemical stimulation
- Conversely, Slick expressed on spinal interneurons facilitates somatostatin-induced itch
- Analgesics targeting Slick channels may decrease pain but could increase itching if they reach the central nervous system

ABSTRACT

Background: Slick, a sodium-activated potassium channel, has been recently identified in somatosensory pathways, but its functional role is poorly understood. The authors of this study hypothesized that Slick is involved in processing sensations of pain and itch.

Methods: Immunostaining, *in situ* hybridization, Western blot, and real-time quantitative reverse transcription polymerase chain reaction were used to investigate the expression of Slick in dorsal root ganglia and the spinal cord. Mice lacking Slick globally (Slick$^{-/-}$) or conditionally in neurons of the spinal dorsal horn (Lbx1-Slick$^{-/-}$) were assessed in behavioral models.

Results: The authors found Slick to be enriched in nociceptive Aδ-fibers and in populations of interneurons in the spinal dorsal horn. Slick$^{-/-}$ mice, but not Lbx1-Slick$^{-/-}$ mice, showed enhanced responses to noxious heat in the hot plate and tail-immersion tests. Both Slick$^{-/-}$ and Lbx1-Slick$^{-/-}$ mice demonstrated prolonged paw licking after capsaicin injection (mean ± SD, 45.6 ± 30.1 s [95% CI, 19.8 to 71.4]; and 13.1 ± 16.1 s [95% CI, 1.8 to 28.0]; $P = 0.006$ [Slick$^{-/-}$ {n = 8} and wild-type {n = 7}, respectively]), which was paralleled by increased phosphorylation of the neuronal activity marker extracellular signal–regulated kinase in the spinal cord. In the spinal dorsal horn, Slick is colocalized with somatostatin receptor 2 (SSTR2), and intrathecal preadministration of the SSTR2 antagonist CYN-154806 prevented increased capsaicin-induced licking in Slick$^{-/-}$ and Lbx1-Slick$^{-/-}$ mice. Moreover, scratching after intrathecal delivery of the somatostatin analog octreotide was considerably reduced in Slick$^{-/-}$ and Lbx1-Slick$^{-/-}$ mice (Slick$^{-/-}$ [n = 8]: 6.1 ± 6.7 bouts [95% CI, 0.6 to 11.7]; wild-type [n =8]: 47.4 ± 51.1 bouts [95% CI, 4.8 to 90.2]; $P = 0.039$).

Conclusions: Slick expressed in a subset of sensory neurons modulates heat-induced pain, while Slick expressed in spinal cord interneurons inhibits capsaicin-induced pain but facilitates somatostatin-induced itch.

(ANESTHESIOLOGY 2022; 136:802–22)

Nociceptive pain serves as an important protective mechanism for drawing attention to potentially injured tissue. It results from the stimulation of nociceptors: sensory neurons with thinly myelinated Aδ-fibers and unmyelinated C-fibers that terminate in the skin or deep tissues. When encountering an acute noxious stimulus (*e.g.*, heat, cold, pressure, chemical stimulation), several ion channels in nociceptors are activated, leading to neuronal depolarization. The information is then transmitted through dorsal root ganglia or trigeminal ganglia into the

Supplemental Digital Content is available for this article. Direct URL citations appear in the printed text and are available in both the HTML and PDF versions of this article. Links to the digital files are provided in the HTML text of this article on the Journal's Web site (www.anesthesiology.org). This article has a visual abstract available in the online version.

Submitted for publication August 22, 2021. Accepted for publication January 31, 2022. Published online first on March 18, 2022.

Cathrin Flauaus, R.Ph.: Institute of Pharmacology and Clinical Pharmacy, Goethe University Frankfurt, Frankfurt am Main, Germany.

Patrick Engel, R.Ph.: Institute of Pharmacology and Clinical Pharmacy, Goethe University Frankfurt, Frankfurt am Main, Germany.

Fangyuan Zhou, M.S.: Institute of Pharmacology and Clinical Pharmacy, Goethe University Frankfurt, Frankfurt am Main, Germany.

Jonas Petersen, Ph.D.: Institute of Pharmacology and Clinical Pharmacy, Goethe University Frankfurt, Frankfurt am Main, Germany.

Peter Ruth, Ph.D.: Department of Pharmacology, Toxicology and Clinical Pharmacy, Institute of Pharmacy, University of Tuebingen, Tuebingen, Germany.

Robert Lukowski, Ph.D.: Department of Pharmacology, Toxicology and Clinical Pharmacy, Institute of Pharmacy, University of Tuebingen, Tuebingen, Germany.

Achim Schmidtko, M.D., Ph.D.: Institute of Pharmacology and Clinical Pharmacy, Goethe University Frankfurt, Frankfurt am Main, Germany.

Ruirui Lu, M.D., Ph.D.: Institute of Pharmacology and Clinical Pharmacy, Goethe University Frankfurt, Frankfurt am Main, Germany.

 Anesthesiology 2022; 136:802–22. DOI: 10.1097/ALN.0000000000004163

dorsal horn of the spinal cord and the brainstem, where the central terminals of nociceptors synapse with intrinsic second-order projection neurons and interneurons. Then the information is conveyed to higher centers in the brain, ultimately resulting in the perception of pain.[1] Similar to pain, itch is also encoded by distinct neurons in both the peripheral and central nervous systems, and the interaction between pain and itch is widely distributed along somatosensory pathways.[2]

Research in the past few decades has revealed that different stimuli are decoded by different subsets of sensory neurons with distinct receptors and ion channels.[3] Potassium channels are emerging targets for understanding this process and developing novel treatments. In general, potassium channels are the most populous and diverse class of neuronal ion channels that are governed by nearly 80 genes in humans.[4] Recently, two distinct potassium channels, both regulated by cytosolic sodium, have attracted significant interest as regulators of pain and itch: Slack (sequence like a Ca^{2+}-activated potassium channel, also termed $K_{Na}1.1$, *Kcnt1*, or *Slo2.2*) and Slick (sequence like an intermediate conductance potassium channel, also termed $K_{Na}1.2$, *Kcnt2*, or *Slo2.1*).[5–8] Slack, which is highly expressed in nonpeptidergic nociceptors, plays an important role in the processing of neuropathic pain and itching, but it seems to have a limited contribution to nociceptive pain sensing.[5,6] Slick has been detected in various regions of the nervous system and in nonneuronal tissues such as the heart, smooth muscle, and pancreatic duct epithelial cells.[6–9] In a previous study addressing the role of Slick in processing pain, Slick immunoreactivity was detected in a population of peptidergic sensory neurons, and Slick knockout mice lacking exons 2 to 7 of the *Kcnt2* gene demonstrated increased sensitivity to noxious heat.[7] Interestingly, a subsequent single-cell RNA-sequencing study detected Slick in dorsal horn neurons and suggested that Slick together with other markers defines 4 of the 15 identified populations of inhibitory interneurons in the dorsal horn.[10] Based on this distribution pattern, we hypothesized that Slick might exert additional functions in somatosensory processing.

Here, we aimed to further characterize the role of Slick in pain and itch processing. We thoroughly assessed the cellular distribution of Slick in neuronal subpopulations in dorsal root ganglia and the spinal dorsal horn by immunostaining and *in situ* hybridization, and we analyzed the pain and itch behavior of global and tissue-specific knockout lines lacking exon 22 of the *Kcnt2* gene.

Materials and Methods

In response to peer review, several experiments were added, including the allyl isothiocyanate test, itch behavior induced by intrathecal injection of 300 ng octreotide, and itch behavior induced by intradermal injection of histamine and chloroquine.

Animals

To generate global Slick knockouts (referred to as $Slick^{-/-}$), Slick floxed ($Slick^{fl/fl}$) mice bearing loxP sites flanking exon 22 of the *Kcnt2* gene (B6(129S4)-*Kcnt2*$^{tm1.1Clin}$/J, JAX stock No. 028419; The Jackson Laboratory, USA)[6] were crossed with cytomegalovirus (CMV)-Cre mice (B6.C-Tg(CMV-cre)1Cgn/J, JAX stock No. 006054, The Jackson Laboratory)[11] and backcrossed with C57BL/6N mice to eliminate the Cre recombinase. Wild-type and $Slick^{-/-}$ mice were obtained from heterozygous breeding. To ablate Slick selectively in dorsal horn neurons, $Slick^{fl/fl}$ mice were crossed with Lbx1-Cre mice[12] to obtain homozygous conditional Slick knockouts (referred to as Lbx1-$Slick^{-/-}$) and control ($Slick^{fl/fl}$) mice. Mice were genotyped by polymerase chain reaction using primer pairs for Kcnt2 (forward: 5′-aactttatgagttcctcttccatg-3′; reverse: 5′-gagcatcatactttgctttttggg-3′; Biomers, Germany) with standard thermocycler amplification conditions using polymerase chain reaction RedMastermix (Genaxxon bioscience, Germany) and an annealing temperature of 60°C. Resulting amplicons were 579 bp for wild-type and 269 bp for $Slick^{-/-}$,[6] and predicted amplicons were 694 bp for Slick-floxed alleles. In addition, Sprague-Dawley rats (Charles River, Germany) were used for immunostaining.

All animals were housed on a 12/12 light/dark cycle with free access to food and water *ad libitum*. Experiments were performed in animals of either sex, but sex had no significant effects in any assay. The total numbers used for each experiment are listed in the Materials and Methods and Results sections, as well as in figure legends, and the numbers of male and female mice are listed in the Materials and Methods. All mice weighed 20 ± 4 g and were a mean age of 12 weeks at the begin of the experiments. Animals were numbered, randomly assigned to different experimental groups according to the experimental strategy, and tested in sequential order. All behavioral tests and anatomical studies, including quantification, were performed by investigators who were blinded to the genotype of the animals. All experiments adhered to the guidelines of the International Association for the Study of Pain, Animal Research: Reporting In Vivo Experiments, and the 3Rs Principles, and were approved by our local Ethics Committee for Animal Research (Regierungspräsidium Darmstadt, Germany).

Real-time Reverse Transcription Polymerase Chain Reaction

Lumbar (L1–L6) dorsal root ganglia, lumbar (L3–L5) spinal cord, and prefrontal cortex of mice ($Slick^{-/-}$: n = 3 [2 females and 1 male]; wild-type: n = 3 [2 females and 1 male]; Lbx1-$Slick^{-/-}$: n = 4 [2 females and 2 males]; control: n = 4 [2 females and 2 males]) were rapidly dissected, snap-frozen in liquid nitrogen, and stored at −80°C until use. Total RNA from spinal cord and cortex was extracted using TRIzol reagent (No. 15596026; Thermo Fisher Scientific,

Germany) or QIAzol lysis reagent (No. 79306; Qiagen, The Netherlands) and chloroform in combination with the RNeasy Mini Kit (No. 74104; Qiagen, The Netherlands) according to the manufacturer's recommendations. Total RNA from dorsal root ganglia was isolated using the innuPREP Micro RNA Kit (No. C-6134; Analytik Jena, Germany) following the manufacturer's instructions.

Isolated RNA was quantified with a NanoDrop 2000 (Thermo Fisher Scientific), and cDNA was synthesized from 200 ng using the first strand cDNA synthesis kit (No. 10774691; Thermo Fisher Scientific) with random hexamer primer. Quantitative real-time reverse transcription polymerase chain reaction was performed on a CFX96 Touch Real-Time System (Bio-Rad, Germany) using the iTaq Universal SYBR Green SuperMix (No. 1725120; Bio-Rad) and primer pairs for Kcnt2 (forward: 5′-gaaagcaccatgagtgcaga-3′, reverse: 5′-gttttgaaagcgcgagagag-3′), Kcnt1 (forward: 5′-ctgctgtgcctggtcttca-3′, reverse: 5′-aaggaggtcagcaggttcaa-3′) and glyceraldehyde 3-phosphate dehydrogenase (forward: 5′-caatgtgtccgtcgtggatct-3′, reverse: 5′-gtcctcagtgtagcccaagatg-3′; all from Biomers, Germany). Reactions were performed in duplicate or triplicate by incubating for 2 min at 50°C and 10 min at 95°C, followed by 40 15-s cycles at 95°C and 60 s at 60°C. Water and template controls were included to ensure specificity. Relative expression of target gene levels was determined using the comparative $2^{-\Delta\Delta Ct}$ method and normalized to glyceraldehyde 3-phosphate dehydrogenase.

Western Blots

For Slick detection, lumbar (L1–L5) dorsal root ganglia and lumbar (L1–L5) spinal cord of Slick$^{-/-}$ and wild-type mice (n = 3 males per group) were rapidly dissected, frozen in liquid nitrogen, and stored at −80°C until use. Lysates were prepared with buffer containing 0.32 M sucrose, 0.1 M NaF, 5 mM sodium phosphate buffer (pH, 7.4 [protocol from University of California–Davis/National Institutes of Health NeuroMab Facility, USA]) mixed with a protease inhibitor cocktail (Complete Mini, No. 4693132001; Roche Diagnostics, Germany). For phosphorylated extracellular signal–regulated kinase (pERK) and ERK detection, lumbar (L4–L5) spinal cord of Slick$^{-/-}$ and wild-type mice (n = 4 per group [1 female and 3 males]) was homogenized in Phosphosafe extraction reagent (No. 71296, Novagen, Germany) mixed with the protease inhibitor cocktail. For somatostatin receptor 2 (SSTR2) detection, the lumbar (L4–L5) spinal cord of Slick$^{-/-}$, wild-type, Lbx1-Slick$^{-/-}$, and control mice (n = 3 per group [1 female and 2 males]) were prepared with radioimmunoprecipitation assay buffer containing 150 mM sodium chloride, 1% Triton X-100, 0.5% sodium deoxycholate, 0.1% sodium dodecyl sulfate, and 50 mM Tris (protocol from Abcam, United Kingdom) mixed with the protease inhibitor cocktail. Extracted proteins (40 to 50 μg per lane) were separated by 6 or 10% SDS-PAGE and blotted onto a nitrocellulose membrane. After blocking of nonspecific binding sites with blocking buffer (Intercept Blocking Buffer, No. 927-70001; LI-COR Bioscience, USA), membranes were incubated with mouse anti-KCNT2/Slo2.1/Slick (1:500, clone N11/33, No. 75-055; NeuroMab, USA), rabbit anti-phospho-p44/42 mitogen-activated protein kinase ([MAPK] Thr202/Tyr204, 1:700, No. 9101S; Cell Signaling, USA), rabbit anti-p44/42 MAPK (Erk1/2; 1:600, No.4695S; Cell Signaling), mouse anti-SSTR2 (1:200, No. sc-365502, Santa Cruz, USA) and mouse anti–α-tubulin (1:1,000; clone DM1A, No. 05-829; Sigma-Aldrich, Germany) dissolved in blocking buffer containing Tween 20, 0.1%, overnight at 4°C. After incubation with secondary antibodies for 1 h at room temperature, proteins were detected using an Odyssey Infrared Imaging System (LI-COR Bioscience). Quantification of band densities was done using Image Studio Lite software (LI-COR Bioscience).

Immunostaining and *In Situ* Hybridization

Mice (n = 5 per group [2 females and 3 males]) and rats (n = 2 females) were killed by carbon dioxide and immediately perfused intracardially with 0.9% saline, followed by 1% or 4% paraformaldehyde in phosphate-buffered saline (pH, 7.4). Lumbar (L3–L5) dorsal root ganglia and lumbar (L3–L5) spinal cord were dissected and cryoprotected in 20% sucrose for 4 h, followed by 30% sucrose overnight. Tissues were frozen in tissue freezing medium (Tissue-Tek O.C.T. Compound, No. 4583; Sakura, USA) on dry ice, cryostat-sectioned at a thickness of 14 μm, and stored at −80°C.

For immunostaining, sections were permeabilized for 5 min in Triton X-100, 0.1%, in phosphate-buffered saline, blocked for 1 h using normal goat serum, 10%, (No. 10000C; Thermo Fisher Scientific) and bovine serum albumin, 3%, (No. A6003; Sigma-Aldrich) in phosphate-buffered saline, and incubated with primary antibodies diluted in 3% bovine serum albumin in phosphate-buffered saline overnight at 4°C or for 2 h at room temperature. The following antibodies were used: mouse anti-Slick (1:500, clone N11/33, No. 75-055; NeuroMab); rabbit anti–calcitonin gene-related peptide ([CGRP] 1:800, No. PC205L; Sigma-Aldrich); guinea pig anti-CGRP (1:600, No. 414 004; Synaptic Systems, Germany); mouse anti-neurofilament 200 ([NF200] 1:2,000, No. N0142; Sigma-Aldrich); rabbit anti-NF200 (1:2,000, No. N4142; Sigma-Aldrich); rabbit anti-transient receptor potential vanilloid 1 ([TRPV1] 1:800, No. ACC-030; Alomone, Israel); and rabbit anti–vesicular glutamate transporter type 3 ([VGLUT3] 1:400, No. 135203; Synaptic Systems). Sections were then washed in phosphate-buffered saline and stained with secondary antibodies conjugated with Alexa Fluor 350, 488, or 555, or Cy5 (1:1,200; all from Thermo Fisher Scientific). For staining of class III β-tubulin (TUBB3), Alexa Fluor 488–conjugated anti-TUBB3 (1:1,000; clone TUJ1, No.

801203; BioLegend, USA) diluted in bovine serum albumin, 3%, in phosphate-buffered saline was incubated for 2 h at 4°C. For staining with *Griffonia simplicifolia* isolectin B4, sections were incubated with Alexa Fluor 488–conjugated isolectin B4 (10 μg/ml in buffer containing 1 mM $CaCl_2 \cdot 2H_2O$, 1 mM $MgCl_2$, 1 mM $MnCl_2$, and Triton X-100, 0.2%; pH, 7.4 [No. 121411; Thermo Fisher Scientific]) for 2 h at room temperature. After immunostaining, slices were immersed for 5 min in 0.06% Sudan black B (No. 199664; Sigma-Aldrich) in 70% ethanol to reduce lipofuscin-like autofluorescence, washed in phosphate-buffered saline, and coverslipped. In double-labeling experiments, primary antibodies were consecutively incubated.

For *in situ* hybridization, we used the QuantiGene ViewRNA tissue assay (Thermo Fisher Scientific), in which target mRNA signals appear as puncta in microscopy. Experiments were performed according to the manufacturer's instructions using a type-1 probe set designed by Thermo Fisher Scientific to the coding region of mouse Slick (Kcnt2; No. VB1-17744) and type-6 probe sets for mouse Slack (Kcnt1; No. VB6-21049), vesicular γ-aminobutyric acid (GABA) transporter ([VGAT] No.VB6-17400), vesicular glutamate transporter 2 (VGLUT2; No. VB6-16625), galanin (GAL; No. VB6-3199892), nitric oxide synthase 1 (nNOS; No.VB6-3197829), neuropeptide Y (NPY; No.VB6-16274), parvalbumin (PVALB; No.VB6-13220), SSTR2 (No. VB6-3201802), and gastrin-releasing peptide receptor ([GRPR] No. VB6-3197053). Controls included scramble type-1 (No.VF1-17155) and type-6 (No. VF6-18580) probe sets. Briefly, tissue sections were fixed in 4% paraformaldehyde for 16 to 18 h at 4°C, dehydrated through 50%, 70%, and 100% ethanol, treated with protease QF for 25 min at 40°C, and incubated with probe sets for 2 h at 40°C. In double *in situ* hybridization experiments, type-1 and type-6 labeled probes were simultaneously incubated. After preamplifier and amplifier hybridization, the signal was developed *via* reaction with fast red and blue substrate (for type-1 and -6 probes, respectively). Finally, sections were costained with 4′,6-diamidino-2-phenylindole (No. D1306; Thermo Fisher Scientific) and mounted with Fluoromount G (No. 00-4958-02; Thermo Fisher Scientific).

Images were taken using an Eclipse Ni-U (Nikon, Germany) microscope equipped with a monochrome charge-coupled device, and were pseudocolored and superimposed. Adjustment of brightness and contrast was done using Adobe Photoshop 2020 software (Adobe Systems, USA). Controls were performed by omitting the first and/or the second primary antibodies, incubating type-1 and type-6 scramble probes, and incubating tissues of $Slick^{-/-}$ mice.

Cell Counting

For quantification of the number of cells expressing Slick or marker, at least three nonadjacent sections per dorsal root ganglia or spinal cords per animal (three mice per genotype) were counted. Only cells showing staining clearly above background were included. The specificity of Slick immunoreactivity was confirmed by simultaneous staining of coembedded tissues of wild-type and $Slick^{-/-}$ mice. The percentage of marker-positive dorsal root ganglia neurons in wild-type and $Slick^{-/-}$ mice is expressed as a proportion of marker-positive cells per total number of dorsal root ganglia neurons. The percentage of Slick-positive dorsal root ganglia neurons that expressed marker was calculated by dividing the number of Slick-positive cells colocalized with marker by the total number of Slick-positive cells. For quantification of mRNA-positive dorsal horn neurons, only nuclei-positive cells with hybridization signals clearly above background were counted.

Behavioral Testing

All behavioral studies were performed with littermate mice. Animals were habituated to the experimental room and randomized to different groups. All experiments were conducted between 9:00 AM and 5:00 PM.

Rotarod Test. Motor coordination was assessed with a Rotarod Treadmill for mice (Ugo Basile, Italy) at a constant rotating speed of 13 rpm. All mice had at least two training sessions before the day of the experiment ($Slick^{-/-}$: n = 16 [7 females and 9 males]; wild-type: n = 16 [9 females and 7 males]; $Lbx1\text{-}Slick^{-/-}$: n = 14 [8 females and 6 males]; control: n = 18 [9 female and 9 males]). The latency to fall was recorded during a maximum period of 120 s. The mean from three latencies was used for analysis.

Hot Plate Test. Mice were individually confined in a Plexiglas chamber on a heated metal surface (Hot/Cold Plate; Ugo Basile, Italy). The time between placement and a nocifensive behavior (shaking or licking of a hind paw, jumping) was recorded, and the animal was removed from the plate immediately after a response. To prevent tissue damage, temperatures of 48°C ($Slick^{-/-}$: n = 12 [6 females and 6 males]; wild-type: n = 12 [5 females and 7 males]; $Lbx1\text{-}Slick^{-/-}$: n = 13 [7 females and 6 males]; control: n = 14 [9 females and 5 males]); 50°C ($Slick^{-/-}$: n = 18 [7 females and 11 males]; wild-type: n = 18 [7 females and 11 males]; $Lbx1\text{-}Slick^{-/-}$: n = 13 [7 females and 6 males]; control: n = 14 [9 females and 5 males]); 52°C ($Slick^{-/-}$: n = 18 [7 females and 11 males]; wild-type: n = 18 [7 females and 11 males]; $Lbx1\text{-}Slick^{-/-}$: n = 12 [6 females and 6 males]; control: n = 12 [7 females and 5 males]); and 54°C ($Slick^{-/-}$: n = 18 [7 females and 11 males]; wild-type: n = 18 [7 females and 11 males]; $Lbx1\text{-}Slick^{-/-}$: n = 12 [6 females and 6 males]; control: n = 12 [7 females and 5 males]) were applied with cutoff times of 80, 40, 30, and 20 s, respectively. Only one test per animal per temperature was performed.

Tail-immersion Test. Mice were immobilized in aluminum foil, which allowed free tail movement. For accommodation, the tip of the tail (approximately one third of the tail length) was first immersed in a water bath (Sunlab D-8810;

neoLab, Germany) at 32°C for 20 s. Then the tip of the tail was immersed in another water bath maintained at 46°C (Slick$^{-/-}$: n = 17 [7 females and 10 males]; wild-type: n = 17 [6 females and 11 males]; Lbx1-Slick$^{-/-}$: n = 16 [9 females and 7 males]; control: n = 16 [8 females and 8 males]); 47°C (Slick$^{-/-}$: n = 18 [12 females and 6 males]; wild-type: n = 18 [9 females and 9 males]; Lbx1-Slick$^{-/-}$: n = 16 [9 females and 7 males]; control: n = 16 [8 females and 8 males]); 48°C (Slick$^{-/-}$: n = 18 [9 females and 9 males]; wild-type: n = 18 [6 females and 12 males]; Lbx1-Slick$^{-/-}$: n = 16 [9 females and 7 males]; control: n = 16 [8 females and 8 males]); 49°C (Slick$^{-/-}$: n = 18 [8 females and 10 males]; wild-type: n = 18 [11 females and 7 males]; Lbx1-Slick$^{-/-}$: n = 16 [9 females and 7 males]; control: n = 16 [8 females and 8 males]); or 50°C (Slick$^{-/-}$: n = 19 [6 females and 13 males]; wild-type: n = 19 [8 females and 11 males]; Lbx1-Slick$^{-/-}$: n = 16 [9 females and 7 males]; control: n = 16 [8 females and 8 males]) with cutoff times of 80, 60, 40, 30, and 20 s, respectively. The latency time to a tail withdrawal reflex was recorded, and the tail was removed from the bath immediately after response.[13] Only one test per animal per temperature was used for analysis.

Cold Plate Test. Mice were individually placed in a Plexiglas chamber on a cold metal surface (Hot/Cold Plate; Ugo Basile) maintained at 10°C or 5°C. The total time the mouse spent lifting the forepaw during a 60-s period was measured *via* stopwatch (Slick$^{-/-}$: n = 12 [8 females and 4 males]; wild-type: n = 11 [6 females and 5 males]).[14] Only one test per animal per temperature was performed.

Cold Plantar Test. Mice were acclimated on a borosilicate glass plate (6.5-mm thickness; GVB GmbH, Germany) in transparent plastic enclosures and acclimated for 40 to 60 min. Powdered dry ice was packed into a modified syringe (3 ml; B. Braun, Germany) with a cut top (1-cm diameter). The open end of the syringe was held against a flat surface while pressure was applied to the plunger to compress the dry ice, and then the dense dry ice pellet was applied to the glass surface underneath a hind paw.[15] The latency to move the paw vertically or horizontally away from the glass plate was measured with a stopwatch. An interval of at least 7 min was allowed between testing separate paws of a single mouse, and an interval of at least 15 min was allowed between trials on any single paw. Three to five measurements per paw were performed (Slick$^{-/-}$: n = 15 [7 females and 8 males]; wild-type: n = 13 [5 females and 8 males]).

Dynamic Plantar Test. Paw withdrawal latency after mechanical stimulation was assessed using a dynamic plantar aesthesiometer (Ugo Basile), which pushes a thin probe (0.5-mm diameter) with increasing force through a wire-gated floor against the plantar surface of the hind paw from beneath. The force increased from 0 to 5 g within 10 s and was then held at 5 g for an additional 10 s.[5] The latency was calculated as the average of four to six exposures with at least 20 s in between (Slick$^{-/-}$: n = 10 [5 females and 5 males]; wild-type: n = 9 [4 females and 5 males]).

Tail-clip Test. Mice were individually placed in a Plexiglass chamber and habituated for 5 min. A plastic clip (force, approximately 300 g; Ericotry, China) was applied on the base of the tail, and the latency to the first response (biting, grasping, or jumping) was recorded (Slick$^{-/-}$: n = 14 [6 females and 8 males]; wild-type: n = 13 [4 females and 9 males]).[16]

Tape-response Test. Mice were individually placed in Plexiglas cylinders and habituated for 5 min. A 3-cm piece of a common laboratory tape (marking tape; Diversified Biotech, USA) was put on the back of the mouse. A response was considered when the mouse stopped moving and bit the piece of tape or showed a visible "wet-dog shake" motion in an attempt to remove the tape.[16] Responses occurring within 5 min were counted (Slick$^{-/-}$: n = 18 [9 females and 9 males]; wild-type: n = 15 [9 females and 9 males]).

Capsaicin Test. Mice were individually confined in a Plexiglas cylinder and habituated for 30 min. Capsaicin (5 μg in 20 μl phosphate-buffered saline containing dimethyl sulfoxide, 2% [Sigma-Aldrich]) was injected into the dorsal surface of a hind paw. The time spent licking the injected paw was recorded with a stopwatch in 1-min intervals during a 20-min period (Slick$^{-/-}$: n = 8 [4 females and 4 males]; wild-type: n = 7 [4 females and 3 males]; Lbx1-Slick$^{-/-}$: n = 8 [3 females and 5 males]; control: n = 9 [6 females and 3 males]). In experiments with the SSTR2 antagonist CYN-154806 (500 ng in 5 μl NaCl, 0.9%; No. C2490; Sigma-Aldrich), the compound was intrathecally administered by direct lumbar puncture under short isoflurane anesthesia 30 min before capsaicin injection into a hind paw (Slick$^{-/-}$: n = 5 [1 female and 4 males]; wild-type: n = 6 [1 female and 5 males]; Lbx1-Slick$^{-/-}$: n = 5 [1 female and 4 males]; control: n = 5 [1 female and 4 males]). The time spent licking the injected paw was recorded during the 20 min after capsaicin injection.

Allyl Isothiocyanate Test. Mice were individually habituated in a Plexiglass cylinder for 30 min. Allyl isothiocyanate (10 nmol in 20 μl phosphate-buffered saline containing dimethyl sulfoxide, 0.05% [Sigma-Aldrich]) was injected into the plantar side of a hind paw. The time spent licking the injected paw was recorded in 5-min intervals up to 30 min after allyl isothiocyanate injection.[17] Mechanical sensitivity was evaluated with a series of von Frey hairs stiffness (0.04 to 2.00 g; Ugo Basile) at 1, 3, 5, and 24 h after allyl isothiocyanate injection (Slick$^{-/-}$: n = 8 [4 females and 4 males]; wild-type: n = 6 [2 females and 4 males]; Lbx1-Slick$^{-/-}$: n = 7 [4 females and 3 males]; control: n = 8 [4 females and 4 males]).

Itch Behavior. Mice were habituated in a Plexiglass cylinder for 30 min. The pruritogens octreotide ([100 ng or 300 ng in 5 μl NaCl, 0.9%; No. O1014; Sigma-Aldrich]; 100 ng octreotide: Slick$^{-/-}$: n = 8 [4 females and 4 males]; wild-type: n = 8 [2 females and 6 males]; Lbx1-Slick$^{-/-}$: n = 8 [6 females and 2 males]; control: n = 8 [4 females and 4 males]; 300 ng octreotide: Slick$^{-/-}$: n = 7 [3 females and 4

males]; wild-type: n = 7 [3 females and 4 males]) or gastrin-releasing peptide (1 nmol in 5 μl NaCl, 0.9% [No. 4011670; Bachem, Switzerland]; Slick$^{-/-}$: n = 8 [4 females and 4 males]; wild-type: n = 8 [4 females and 4 males]) were intrathecally administered by direct lumbar puncture under short isoflurane anesthesia. The pruritogens histamine (200 μg in 10 μl NaCl, 0.9% [No. H7125; Sigma-Aldrich]; Lbx1-Slick$^{-/-}$: n = 5 [3 females and 2 males]; control: n = 6 [2 females and 4 males]) and chloroquine (200 μg in 10 μl NaCl, 0.9% [No. C6628; Sigma-Aldrich]; Lbx1-Slick$^{-/-}$: n = 5 [3 females and 2 males]; control: n = 6 [2 females and 4 males]) were injected intradermally into the nape of the neck. The number of scratching bouts that occurred during a 30-min period was recorded using a video tracking system (VideoMot; TSE Systems, Germany) without human presence in the experiment room.[18]

Statistical Analysis

Statistical analysis was performed with GraphPad Prism software version 8.0 (GraphPad, USA). No statistical power calculation was conducted before the study, and the sample sizes were determined based on our previous knowledge and experience with this design. Group sizes and experimental units are indicated in the Materials and Methods and Results sections, as well as figure legends. No outliers were observed, and no data were excluded from statistical analysis. Rotarod fall-off latencies were analyzed with Mann–Whitney U test and are expressed as medians and interquartile ranges. All other data are presented as mean ± SD. For some data, 95% CI are reported in the Results section, and *t* or F values are reported in the figure legends. Differences between two groups (*e.g.,* responses to the hot plate, tail-immersion, cold plate, cold plantar, dynamic plantar, tail-clip, and tape test; sum of licking time after allyl isothiocyanate injection; sum of scratching bouts after injection of histamine and chloroquine) were determined using two-tailed, unpaired *t* tests. Differences in Slack mRNA expression, dorsal root ganglia neurons subpopulations, Slick mRNA expression, sum of licking time after capsaicin, and Western blots of phosphorylated extracellular signal-regulated kinase and extracellular signal-regulated kinase, and sum of scratching bouts after injection of octreotide with two doses were determined using multiple *t* tests. Allyl isothiocyanate–induced mechanical hypersensitivity was determined using two-way repeated-measures ANOVA followed by the *post hoc* Sidak multiple comparison test. For all tests, $P < 0.05$ was considered as statistically significant.

Results

Slick Is Expressed in Aδ-Fiber Nociceptors and Dorsal Horn Interneurons

To study the functions of Slick potassium channels in pain processing, we first produced mice lacking Slick globally by crossing a mouse strain containing exon 22 of the *Kcnt2* gene flanked by two loxP sites[6] with transgenic mice expressing Cre under the transcriptional control of the cytomegalovirus promotor.[11] The resulting knockout mice (referred to as Slick$^{-/-}$) were viable and fertile, and in accordance with previous studies, there were no obvious differences in gross appearance and general behavior among Slick$^{-/-}$ and wild-type littermates.[6] The deletion of Slick was confirmed by Western blotting in tissue extracts from dorsal root ganglia and the spinal cord (n = 3 per group; fig. 1A). The mRNA expression of Slack, a paralogous potassium channel that has been reported to form heteromers with Slick,[19] was unaltered in dorsal root ganglia (Slick$^{-/-}$ [n = 3]: 0.8 ± 0.2 [95% CI, 0.4 to 1.3]; wild-type [n = 3]: 1.0 ± 0.1 [95% CI, 0.8 to 1.2]; $P = 0.163$; fig. 1B) and the spinal cord of Slick$^{-/-}$ mice (Slick$^{-/-}$ [n = 3]: 0.5 ± 0.0 [95% CI, 0.4 to 0.6]; wild-type [n = 3]: 0.5 ± 0.1 [95% CI, 0.2 to 0.8]; $P > 0.999$; fig. 1B). Moreover, the overall frequencies of dorsal root ganglia neuron populations positive for the established markers isolectin B4 (Slick$^{-/-}$ [n = 3]: 29.8 ± 3.6% [95% CI, 20.8 to 38.9%]; wild-type [n = 3]: 31.4 ± 2.4% [95% CI, 25.5 to 37.3%]; $P = 0.920$; fig. 1C); CGRP (Slick$^{-/-}$ [n = 3]: 33.0 ± 8.6% [95% CI, 11.8 to 54.3%]; wild-type [n = 3]: 39.6 ± 1.0% [95% CI, 37.0 to 42.2%]; $P = 0.371$; fig. 1C); and NF200 (Slick$^{-/-}$ [n = 3]: 58.3 ± 0.8% [95% CI, 56.2 to 60.4%]; wild-type [n = 3]: 58.5 ± 8.0% [95% CI, 38.7 to 78.3%]; $P = 0.953$; fig. 1C) were similar between genotypes, suggesting that there are no general defects in Slick$^{-/-}$ mice.

We then analyzed the cellular distribution of Slick in dorsal root ganglia by immunostaining and detected Slick immunoreactivity in a population of sensory neurons of wild-type mice (fig. 1D). Costaining with the pan-neuronal marker TUBB3 revealed that 9.3 ± 4.2% of total dorsal root ganglia neurons in wild-type mice expressed Slick (n = 4 per group; fig. 1D). No Slick immunoreactivity was seen in dorsal root ganglia from Slick$^{-/-}$ mice (fig. 1E), validating the specificity of our Slick antibody–based staining protocol. In further costaining experiments, we found that the vast majority (91.5 ± 12.0%) of Slick-positive (Slick^{+}) cells expressed CGRP, a marker of the peptidergic population of nociceptors (fig. 1, F and H), confirming a previous report.[7] Conversely, 36.3 ± 25.1% of CGRP^{+} cells coexpressed Slick, suggesting that Slick is localized to only a fraction of CGRP^{+} cells. Interestingly, 93.9 ± 8.6% of Slick^{+} cells were immunoreactive for NF200, which labels myelinated dorsal root ganglia neurons, and 90.2 ± 13.8% of Slick^{+} cells expressed both CGRP and NF200 (n = 5 per group; fig. 1, F and H). This finding implicates that Slick is mainly localized to thinly myelinated Aδ-fiber nociceptors, which are CGRP^{+} and NF200^{+}.[20–22] This subclass of dorsal root ganglia neurons has recently been classified as peptidergic 2 (PEP2) neurons in a single-cell RNA-sequencing study.[23]

Slick immunostaining was virtually absent from sensory neurons binding isolectin B4, a marker of nonpeptidergic unmyelinated C-fiber nociceptors (n = 5 per

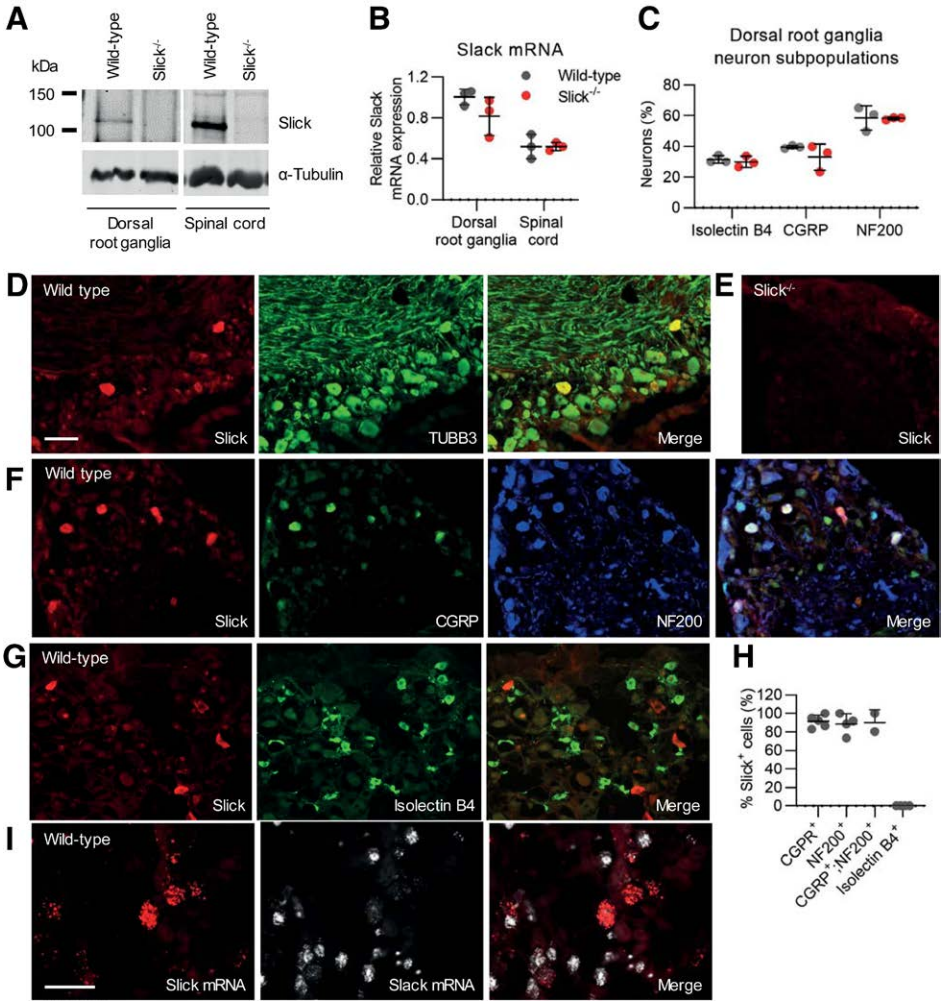

Fig. 1. Distribution of Slick in dorsal root ganglia. (*A*) Western blot analysis of Slick (130 kDa) in dorsal root ganglia and spinal cord from wild-type and Slick$^{-/-}$ mice. Slick was specifically detected in tissues of wild-type, but not Slick$^{-/-}$, mice. α-Tubulin (55 kd) was used as loading control. (*B*) Quantitative reverse transcription polymerase chain reaction in dorsal root ganglia and the spinal cords of wild-type and Slick$^{-/-}$ mice revealed that Slack mRNA expression is not compensatory regulated in the absence of Slick (dorsal root ganglia: $t_8 = 1.96$, $P = 0.163$; spinal cord: $t_8 = 0.00$, $P > 0.999$; n = 3 per group). Values were normalized to wild-type dorsal root ganglia. (*C*) Percentages of dorsal root ganglia neurons that are isolectin B4–binding or immunoreactive for calcitonin gene-related peptide (CGRP) or neurofilament 200 (NF200) are comparable between wild-type and Slick$^{-/-}$ mice (isolectin B4: $t_{12} = 0.37$, $P = 0.920$; CGRP: $t_{12} = 1.57$, $P = 0.371$; NF200: $t_{12} = 0.06$, $P = 0.953$; n = 3 per group). (*D*) Double-immunostaining of Slick with the pan-neuronal marker class III β-tubulin (TUBB3) in dorsal root ganglia of wild-type mice reveals Slick expression in 9.3 ± 2.4% of TUBB3-positive dorsal root ganglia neurons (892 neurons counted; n = 4 per group). (*E*) No Slick immunoreactivity was detected in dorsal root ganglia of Slick$^{-/-}$ mice, confirming the specificity of the anti-Slick antibody. (*F*) Triple-immunostaining of Slick with CGRP and NF200 shows that Slick is mainly localized to dorsal root ganglia neurons that are positive for both CGRP and NF200 (*i.e.,* are in myelinated Aδ nociceptors). (*G*) Double-labeling of Slick and isolectin B4 shows that Slick is absent from isolectin B4–binding dorsal root ganglia neurons. (*H*) Percentage of marker-positive neurons that coexpress Slick (5,959 cells counted; n = 5 per group). (*I*) Double *in situ* hybridization of Slick mRNA with Slack mRNA confirms that Slick and Slack are not coexpressed in dorsal root ganglia neurons. Data are shown as mean ± SD. Scale bars = 50 μm.

group; fig. 1, G and H). Considering that Slack is nearly exclusively expressed in isolectin B4–binding nociceptors,[5] this observation suggests that Slick and Slack do not form heteromers in dorsal root ganglia neurons, unlike in other tissues.[6,24] Indeed, double-labeling fluorescent *in situ* hybridization confirmed that Slick and Slack mRNA do not overlap in dorsal root ganglia neurons (n = 3 per group; fig. 1I). Furthermore, a similar distribution pattern of Slick with enrichment in CGRP$^+$;NF200$^+$ cells and absence from isolectin B4–binding cells was observed in dorsal root ganglia from rats (Supplemental Digital Content 1 fig. 1, http://links.lww.com/ALN/C805). Together, these analyses of dorsal root ganglia tissues indicate that Slick is mainly expressed in Aδ-fiber nociceptors.

We next assessed the distribution of Slick in the spinal cord and observed profound immunoreactivity in the superficial dorsal horn of wild-type mice (fig. 2A, left). Control experiments confirmed that Slick immunoreactivity was absent in the spinal cord of Slick$^{-/-}$ mice (fig. 2A, right). Inconsistent with the expression pattern of Slick in dorsal root ganglia neurons, Slick immunoreactivity in the dorsal horn was not limited to the central terminals of Aδ-fibers that terminate mainly in lamina I and V.[25] Colabeling experiments revealed that Slick immunoreactivity is present in lamina I and outer lamina II (marked by CGRP staining; fig. 2B), in the dorsal region of inner lamina II (marked by isolectin B4 binding; fig. 2C), and in the ventral region of inner lamina II (marked by VGLUT3 staining; fig. 2D).[26] These observations, together with available single-cell RNA-sequencing data,[10] suggest that in addition to dorsal root ganglia neurons, populations of intrinsic neurons in the dorsal horn express Slick.

To further investigate the expression of Slick in the spinal dorsal horn, we performed fluorescent *in situ* hybridization experiments of Slick mRNA. Consistent with the protein expression pattern previously described (fig. 2), multiple hybridization signals were detected in the dorsal horn (fig. 3A, left). As our hybridization probe (which binds to nucleotides 624 to 1568 of Slick mRNA, corresponding to exons 8 through 16) cannot distinguish between tissues from wild-type and Slick$^{-/-}$ mice (in which exon 22 is deleted), we used a scramble probe as a specificity control (fig. 3A, right). To estimate the distribution of Slick in inhibitory and excitatory interneurons of the superficial dorsal horn, we performed double-labeling *in situ* hybridization of Slick mRNA with VGAT mRNA, a marker of inhibitory neurons, and VGLUT2 mRNA, which marks excitatory neurons.[10] We found that 67.3 ± 2.5% of Slick^{+} cells in the superficial dorsal horn expressed VGAT (fig. 3B), whereas 28.7 ± 8.8% of Slick^{+} cells were positive for VGLUT2 (fig. 3C). Conversely, 69.8 ± 4.5% of VGAT^{+} neurons and 21.5 ± 5.6% of VGLUT2^{+} neurons in the superficial dorsal horn express Slick (fig. 3, B and C). These data indicate that Slick is predominantly, but not exclusively, expressed in inhibitory interneurons of the superficial dorsal horn of the spinal cord.

We then further analyzed the cellular distribution of Slick in subpopulations of inhibitory interneurons in the dorsal horn. Previous studies have identified five largely nonoverlapping neurochemical populations that express GAL, nNOS, NPY, PVALB, and calretinin.[25] We found that 38.4 ± 5.7%, 11.9 ± 2.8%, and 10.8 ± 2.7% of Slick^{+} cells coexpressed GAL, nNOS, and NPY, respectively (fig. 3, D to F). Conversely, 80.2 ± 1.1% of GAL^{+}, 49.5 ± 4.8% of nNOS^{+}, and 25.4 ± 8.8% of NPY^{+} neurons coexpressed Slick (fig. 3, D to F). By contrast, there was virtually no colocalization of Slick with PVALB (fig. 3G). We did not analyze the colocalization of Slick and calretinin, because this marker is also significantly expressed by excitatory interneurons.[27] Altogether, the localization in distinct populations of dorsal horn neurons in combination with the enrichment in Aδ-fiber nociceptors supports the idea that Slick is involved in somatosensory processing.

Slick$^{-/-}$ Mice Display Increased Heat Sensitivity but Normal Cold and Mechanical Sensitivity

To assess the functional relevance of Slick for somatosensory processing, we tested the sensitivity of Slick$^{-/-}$ and littermate wild-type mice to various innocuous and noxious sensory stimuli. As a prerequisite for behavioral testing, we first characterized their motor coordination and balance using the rotarod test. Slick$^{-/-}$ and wild-type mice demonstrated intact motor coordination, as analyzed in the rotarod test (median fall-off latencies: Slick$^{-/-}$ [n = 16]: 120 s [interquartile range, 108.0 to 120.0]; wild-type [n = 16]: 120 s [interquartile range, 120.0 to 120.0]; P = 0.174), suggesting that Slick$^{-/-}$ mice are suitable for behavioral analyses. We then tested the ability of Slick$^{-/-}$ mice to respond to heat. In the hot plate test, Slick$^{-/-}$ mice exhibited significantly shorter latencies than wild-type mice when the plate was set at 48°C (Slick$^{-/-}$ [n = 12]: 29.3 ± 11.0 s [95% CI, 22.3 to 36.3]; wild-type [n = 12]: 47.3 ± 17.8 s [95% CI, 36.0 to 58.6]; P = 0.007) and 50°C (Slick$^{-/-}$ [n = 18]: 22.1 ± 9.0 s [95% CI, 17.6 to 26.6]; wild-type [n = 18]: 28.6 ± 6.0 s [95% CI, 25.6 to 31.5]; P = 0.015), but they responded normally at higher temperatures of 52°C (Slick$^{-/-}$ [n = 18]: 15.6 ± 6.3 s [95% CI, 12.5 to 18.8]; wild-type [n = 18]: 18.4 ± 4.8 s [95% CI, 16.0 to 20.7]; P = 0.149) and 54°C (Slick$^{-/-}$ [n = 18]: 8.5 ± 2.5 s [95% CI, 7.3 to 9.7]; wild-type [n = 18]: 10.1 ± 3.3 s [95% CI, 8.4 to 11.7]; P = 0.122; fig. 4A; results for female and male cohorts are shown in Supplemental Digital Content 2 fig. 2, A and B, http://links.lww.com/ALN/C806). Similarly, in the tail-immersion assay, Slick$^{-/-}$ animals showed significantly shorter tail flick latencies compared with wild-type littermates for bath temperatures of 46°C (Slick$^{-/-}$ [n = 17]: 20.1 ± 13.0 s [95% CI, 13.4 to 26.8]; wild-type [n = 17]: 32.7 ± 19.0 s [95% CI, 22.9 to 42.4]; P = 0.032), 47°C (Slick$^{-/-}$ [n = 18]: 7.6 ± 3.5 s [95% CI, 5.9 to 9.3]; wild-type [n = 18]: 11.4 ± 5.3 s [95% CI, 8.7 to 14.0]; P = 0.016), and 48°C (Slick$^{-/-}$ [n = 18]: 5.0 ± 2.0 s [95% CI, 4.0 to 6.0]; wild-type [n = 18]: 7.1 ± 2.1 s [95% CI, 6.0 to 8.1]; P = 0.004), whereas responses to the higher temperatures 49°C (Slick$^{-/-}$ [n = 18]: 3.1 ± 1.7 s [95% CI, 2.2 to 3.9]; wild-type [n = 18]: 7.1 ± 2.1 s [95% CI, 3.3 to 4.3]; P = 0.107) and 50°C (Slick$^{-/-}$ [n = 19]: 2.5 ± 1.0 s [95% CI, 2.1 to 3.0]; wild-type [n = 19]: 3.0 ± 1.6 s [95% CI, 2.2 to 3.7]; P = 0.323) were unaltered (fig. 4B; results for female and male cohorts are presented in Supplemental Digital Content 2 fig. 2, C to E, http://links.lww.com/ALN/C806). These data suggest that Slick specifically controls heat sensation at distinct temperatures.

We next analyzed cold sensitivity of Slick$^{-/-}$ and wild-type littermates. In the cold plate test, the duration of forepaw lifting[14] at either 10°C or 5°C was comparable between

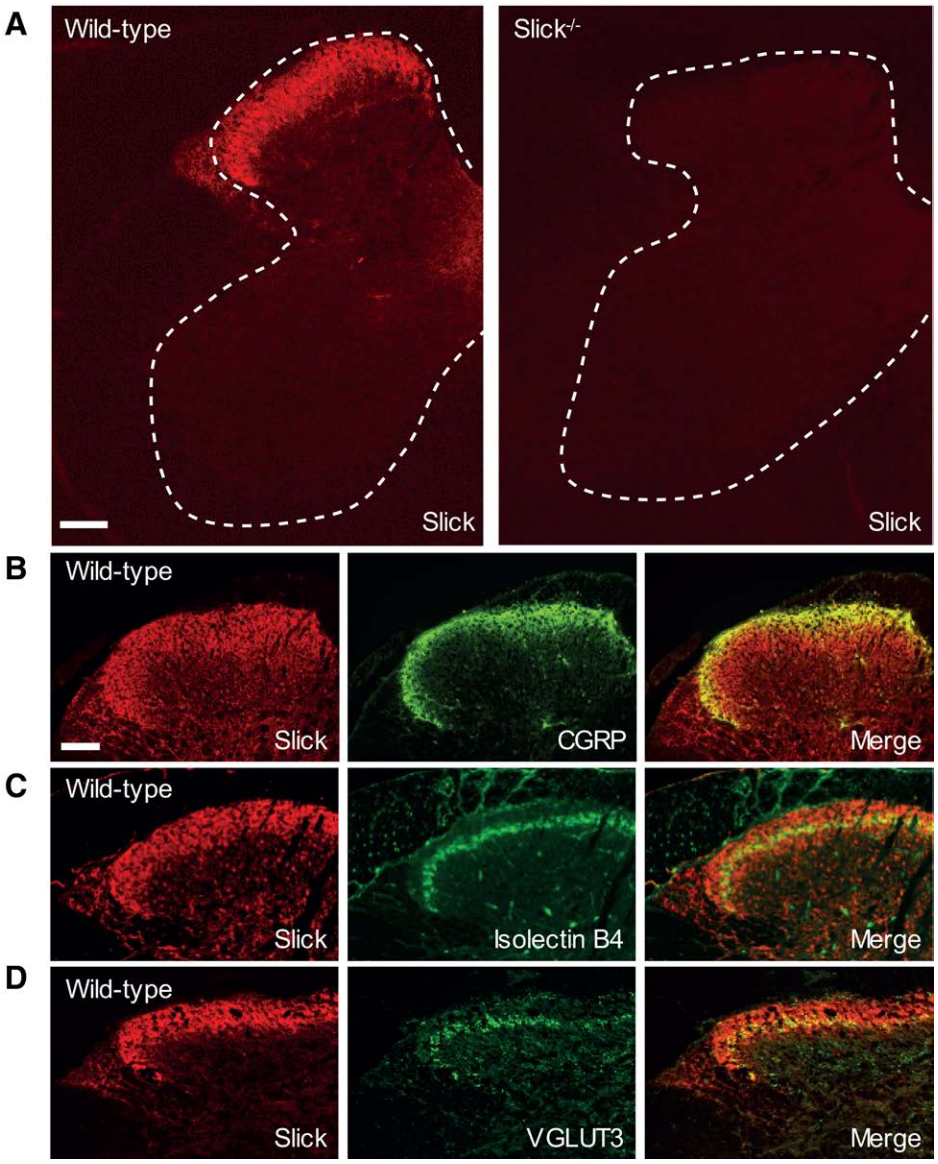

Fig. 2. Distribution of Slick protein in the spinal cord. (*A*) Immunostaining of Slick in the lumbar spinal cord of wild-type (*left*) and Slick$^{-/-}$ (*right*) mice reveals specific Slick expression in the superficial dorsal horn. Dotted lines delineate the gray matter. (*B* through *D*) Double-labeling of Slick with calcitonin gene-related peptide ([CGRP] which labels lamina I and outer lamina II [*B*]), isolectin B4 (inner/dorsal region of lamina II [*C*]), and vesicular glutamate transporter type 3 ([VGLUT3] inner/ventral region of lamina II [*D*]) shows that Slick immunoreactivity expands from lamina I to the ventral part of inner lamina II. Scale bars = 100 μm.

genotypes (10°C: Slick$^{-/-}$ [n = 12]: 16.2 ± 8.7 s [95% CI, 10.6 to 21.7]; wild-type [n = 11]: 16.9 ± 7.5 s [95% CI, 11.9 to 21.9]; P = 0.915; 5°C: Slick$^{-/-}$ [n = 12]: 39.5 ± 13.1 s [95% CI, 31.1 to 47.8]; wild-type [n = 11]: 41.0 ± 8.5 s [95% CI, 35.3 to 46.7]; P = 0.915; fig. 4C). Similar to the cold plate test, Slick$^{-/-}$ mice showed normal latencies in the cold plantar test (Slick$^{-/-}$ [n = 15]: 11.6 ± 2.0 s [95% CI, 10.5 to 12.7]; wild-type [n = 13]: 11.8 ± 2.4 s [95% CI, 10.4 to 13.2]; P = 0.814; fig. 4D), in which a dry ice pellet is pushed to a glass surface beneath the hind paw.[15] These data suggest an unimpaired cold sensitivity in the absence of Slick. In tests of mechanosensitivity, Slick$^{-/-}$ mice showed normal withdrawal latencies to an increasing mechanical force applied to the hind paw with a dynamic plantar aesthesiometer (Slick$^{-/-}$ [n = 10]: 9.1 ± 0.9 s [95% CI, 8.4 to 9.7]; wild-type [n = 9]: 9.1 ± 0.7 s [95% CI, 8.6 to 9.6 s]; P = 0.956; fig. 4E). They also demonstrated unaltered responses to a noxious mechanical stimulus in the tail-clip test (Slick$^{-/-}$ [n = 14]: 6.7 ± 7.0 s [95% CI, 2.7 to 10.7]; wild-type [n =13]: 6.8 ± 6.0 s [95% CI, 3.1 to 10.4];

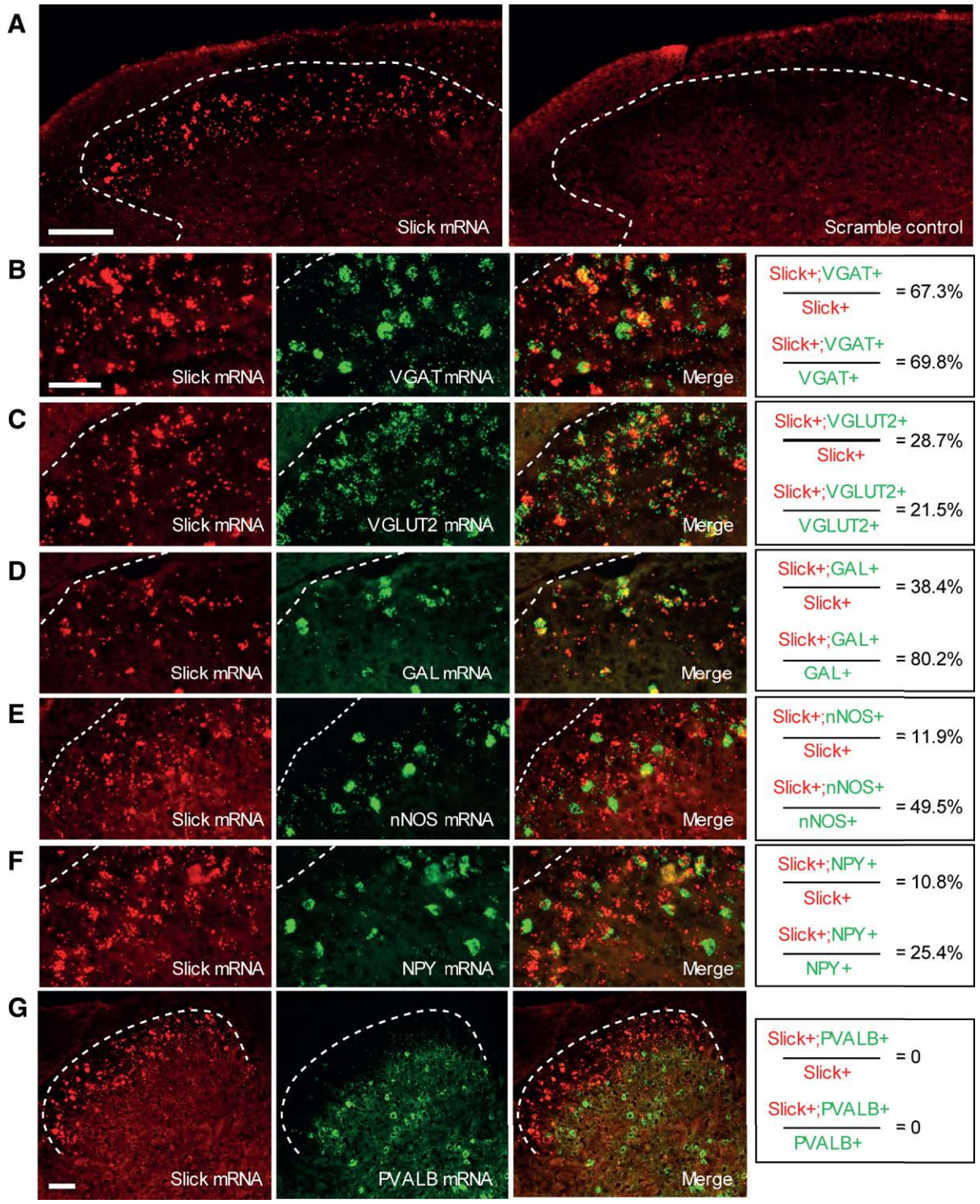

Fig. 3. Expression of Slick mRNA in the spinal dorsal horn. (*A*) Distribution of Slick mRNA (*left*) in the dorsal horn of the spinal cord assessed by fluorescent *in situ* hybridization. No hybridization signal was detected using a scramble control (*right*). (*B* and *C*) Double *in situ* hybridization of Slick mRNA with mRNA of VGAT (*B*), a marker of inhibitory interneurons, and of VGLUT2 (*C*), a marker of excitatory interneurons. (*D* through *G*) Double *in situ* hybridization of Slick mRNA with mRNA of galanin (GAL; *D*), neuronal nitric oxide synthase (nNOS; *E*), neuropeptide Y (NPY; *F*), and parvalbumin (PVALB; *G*), which mark subpopulations of inhibitory interneurons. The percentage of Slick$^+$ neurons that coexpress the selected marker and the percentage of marker-positive neurons that coexpress Slick are presented in the column (*right*). Scale bar = 100 μm (*A*); scale bars = 50 μm (*B* and *G*).

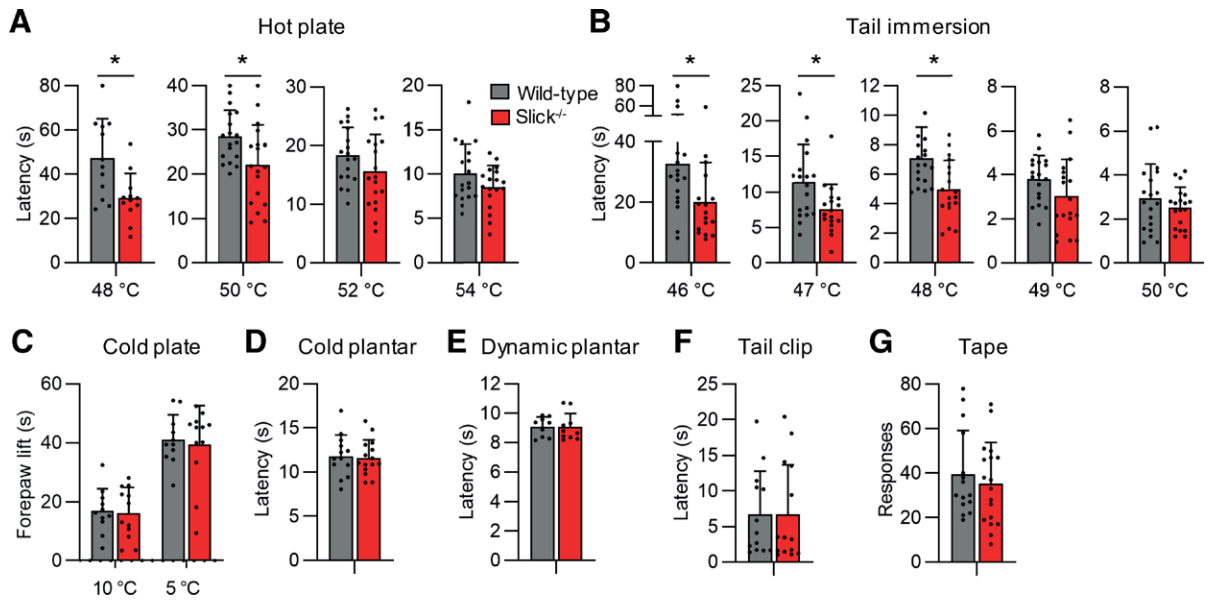

Fig. 4. Behavioral responses of Slick$^{-/-}$ mice to heat, cold, and mechanical stimuli. (*A* and *B*) Responses to heat stimuli. (*A*) In the hot plate test, Slick$^{-/-}$ mice showed significantly reduced latencies compared with wild-type mice at 48° and 50°C, but showed unaltered responses at 52° and 54°C (48°C [n = 12 per group]: $t_{22} = 2.99$, $P = 0.007$; 50°C [n = 18 per group]: $t_{34} = 2.55$, $P = 0.015$; 52°C [n = 18 per group]: $t_{34} = 1.48$, $P = 0.149$; 54°C [n = 18 per group]: $t_{34} = 1.58$, $P = 0.122$). (*B*) In the tail-immersion test, tail withdrawal latencies were significantly reduced in Slick$^{-/-}$ mice compared with wild-type mice at 46°C ($t_{32} = 2.24$, $P = 0.032$; n = 17 per group), 47°C ($t_{34} = 2.53$, $P = 0.016$; n = 18 per group), and 48°C ($t_{34} = 3.05$, $P = 0.004$; n = 18 per group), but were normal at 49°C ($t_{34} = 1.65$, $P = 0.107$; n = 18 per group) and 50°C ($t_{36} = 1.00$, $P = 0.323$; n = 19 per group). (*C* and *D*) Responses to cold stimuli. (*C*) On a cold plate maintained at 10°C or 5°C, the duration of forepaw lifting within 1 min was comparable between groups (10°C: $t_{21} = 0.22$, $P = 0.831$; n = 12 [Slick$^{-/-}$], n = 11 [wild-type]; 5°C: $t_{21} = 0.33$, $P = 0.744$; n = 12 [Slick$^{-/-}$], n = 11 [wild-type]). (*D*) Paw withdrawal latencies in the cold plantar test were similar between groups ($t_{26} = 0.24$, $P = 0.814$; n = 15 [Slick$^{-/-}$], n = 13 [wild-type]). (*E* through *G*) Responses to mechanical stimuli. Slick$^{-/-}$ mice showed normal responses to mechanical stimuli in the dynamic plantar test ([*E*] $t_{17} = 0.06$, $P = 0.956$; n = 10 [Slick$^{-/-}$], n = 9 [wild-type]); tail-clip test ([*F*] $t_{25} = 0.02$, $P = 0.982$; n = 14 [Slick$^{-/-}$], n = 13 [wild-type]) and tape response test ([*G*] $t_{31} = 0.64$, $P = 0.526$; n = 18 [Slick$^{-/-}$], n = 15 [wild-type]). Data are presented as mean ± SD. *$P < 0.05$.

$P = 0.982$; fig. 4F) and to innocuous mechanical stimuli evoked by applying an adhesive tape to the hairy skin of the back (Slick$^{-/-}$ [n = 18]: 35.3 ± 18.5 s [95% CI, 26.1 to 44.5]; wild-type [n = 15]: 39.5 ± 19.6 s [95% CI, 28.7 to 50.4]; $P = 0.526$; fig. 4G). Altogether, these behavioral assays implicate a specific alteration of noxious heat sensation in Slick$^{-/-}$ mice.

Slick in the Spinal Dorsal Horn Is Dispensable for Heat Sensation

Given the significant expression of Slick in dorsal horn neurons, we aimed to assess to what extent Slick in intrinsic spinal cord neurons contributes to pain processing. For that purpose, we crossed Lbx1-Cre mice, in which Cre is mainly restricted to neurons of the dorsal spinal cord and the dorsal hindbrain,[12] with Slick$^{fl/fl}$ mice. In the resulting conditional knockouts (referred to as Lbx1-Slick$^{-/-}$), Slick mRNA expression in the spinal cord was significantly downregulated as compared to control (Slick$^{fl/fl}$) mice (Lbx1-Slick$^{-/-}$ [n = 4]: 0.3 ± 0.0 [95% CI, 0.2 to 0.3]; control [n = 4]: 0.9 ± 0.0 [95% CI, 0.9 to 0.9]; $P < 0.001$; fig. 5A), whereas Slick mRNA expression was unaltered in dorsal root ganglia (Lbx1-Slick$^{-/-}$ [n = 4]: 0.9 ± 0.1 *vs.* 1.0 ± 0.1; $P = 0.420$; fig. 5A) or brain cortex (Lbx1-Slick$^{-/-}$ [n = 4] *vs.* control [n = 4]: 4.0 ± 0.2 *vs.* 3.7 ± 0.3; $P = 0.122$; fig. 5A). Immunostainings confirmed a considerable reduction of Slick immunoreactivity in the spinal dorsal horn of Lbx1-Slick$^{-/-}$ mice (fig. 5B), and the antibody specificity was confirmed by staining of Slick$^{-/-}$ tissues (fig. 5B). The expression of Slack mRNA in dorsal root ganglia, the spinal cord and brain cortex was not compensatory regulated in Lbx1-Slick$^{-/-}$ mice (Lbx1-Slick$^{-/-}$ [n = 4] *vs.* control [n = 4]: dorsal root ganglia: 2.4 ± 0.3 *vs.* 2.1 ± 0.3; $P = 0.218$; spinal cord: 1.1 ± 0.2 *vs.* 1.0 ± 0.1; $P = 0.816$; cortex: 1.1 ± 0.3 *vs.* 1.0 ± 0.3; $P = 0.816$; fig. 5C). Furthermore, in the rotarod test, Lbx1-Slick$^{-/-}$ and control mice demonstrated intact motor coordination, as analyzed in the rotarod test (median fall-off latencies: Lbx1-Slick$^{-/-}$ [n = 14]: 120 s [interquartile range, 120.0 to 120.0]; control [n = 18]: 120 s [interquartile range, 120.0 to 120.0]; $P = 0.806$), indicating intact motor coordination and balance.

We then tested heat, cold, and mechanical sensations in Lbx1-Slick$^{-/-}$ mice. Unlike Slick$^{-/-}$ mice, the responses to acute heat stimuli in the hot plate (Lbx1-Slick$^{-/-}$ [n = 13] *vs.* control [n = 14]: 48°C: 48.5 ± 18.4 s *vs.* 51.3 ± 14.8 s; $P = 0.661$; 50°C: 27.4 ± 7.6 s *vs.* 25.2 ± 4.7 s; $P = 0.383$; and Lbx1-Slick$^{-/-}$ [n = 12] *vs.* control [n = 12]: 52°C: 18.2 ± 4.0 s *vs.* 18.9 ± 3.5 s; $P = 0.665$; 54°C, 12.1 ± 2.6 s *vs.* 11.2 ± 3.1 s; $P = 0.431$) and tail immersion test (Lbx1-Slick$^{-/-}$ [n = 16] *vs.* control [n = 16]: 46°C: 13.8 ± 8.1 s *vs.* 14.8 ± 7.6 s; $P = 0.640$; 47°C: 5.5 ± 2.4 s *vs.* 8.0 ± 4.6 s; $P = 0.496$; 48°C: 3.4 ± 1.5 s *vs.* 3.4 ± 2.0 s; $P = 0.942$; 49°C: 2.0 ± 0.8 s *vs.* 1.7 ± 0.5 s; $P = 0.856$) were unaltered in Lbx1-Slick$^{-/-}$ mice (fig. 5, D and E). Moreover, similar to Slick$^{-/-}$ mice, Lbx1-Slick$^{-/-}$ mice demonstrated normal responses to cold and mechanical stimuli (cold plate, cold plantar, dynamic plantar, tail-clip, and tape-response test: data not shown). These data suggest that Slick in dorsal horn neurons is dispensable for the immediate behavioral responses to acute heat, cold, and mechanical stimuli.

Slick in the Spinal Dorsal Horn Modulates Capsaicin-induced Behavior

We then analyzed the tonic pain behavior of Slick$^{-/-}$ and wild-type mice using the capsaicin test. Intraplantar injection of capsaicin (5 μg) into a hind paw elicits a robust paw licking behavior that typically lasts for a few minutes and is mainly driven by TRPV1 activation.[28] As shown in figure 6A, the paw licking response was similar in Slick$^{-/-}$ and wild-type mice during the first 5 min after the capsaicin injection (Slick$^{-/-}$ [n = 8]: 27.0 ± 11.1 s [95% CI, 17.7 to 36.4]; wild-type [n = 7]: 21.4 ± 7.7 s [95% CI, 14.3 to 28.5]; $P = 0.574$). Interestingly however, Slick$^{-/-}$ mice continued to lick the paw during 6 to 20 min after the capsaicin injection, while this late-stage licking behavior was virtually absent in wild-type mice. The sum of licking time during the 6 to 20 min period was significantly increased in Slick$^{-/-}$ mice compared with wild-type mice (Slick$^{-/-}$ [n = 8]: 45.6 ± 30.1 s [95% CI, 19.8 to 71.4]; wild-type [n = 7]: 13.1 ± 16.1 s [95% CI, –1.8 to 28.0]; $P = 0.006$; fig. 6A; results for female and male cohorts are presented in Supplemental Digital Content 3 fig. 3, A and B, http://links.lww.com/ALN/C807), suggesting that Slick controls the nocifensive behavior at late stages of the capsaicin test.

We then exposed Lbx1-Slick$^{-/-}$ mice to capsaicin injection. Notably, similar to Slick$^{-/-}$ mice, the licking behavior in Lbx1-Slick$^{-/-}$ mice was enhanced in the later phase, *i.e.*, 6 to 20 min after capsaicin injection (Lbx1-Slick$^{-/-}$

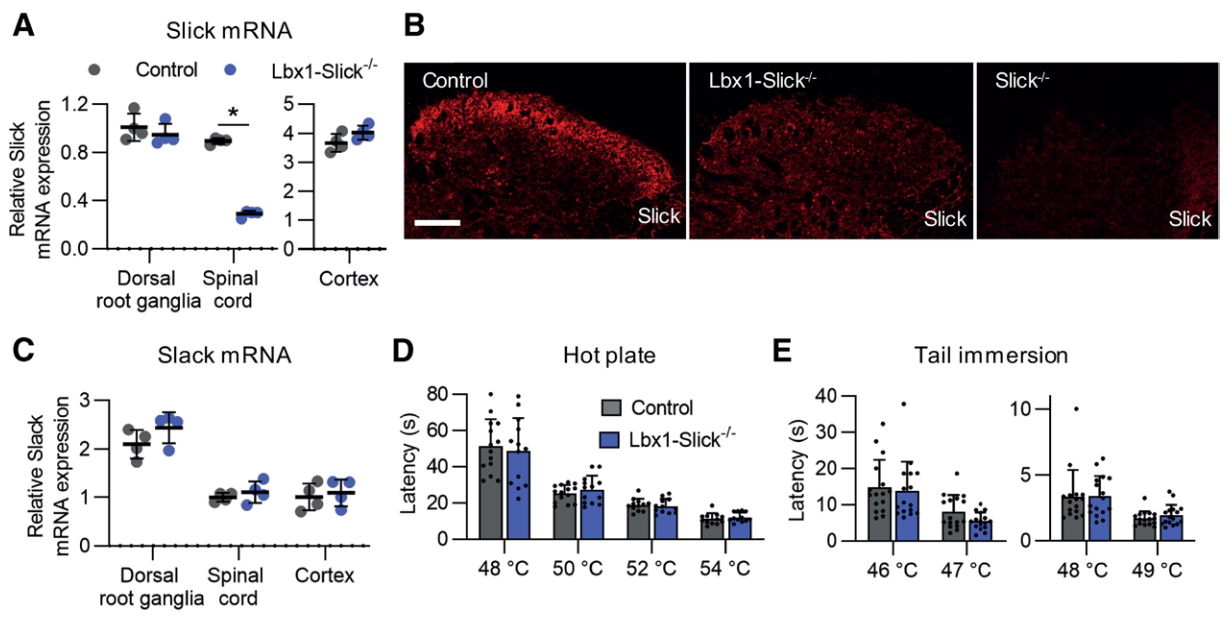

Fig. 5. Lbx1-Slick$^{-/-}$ mice show normal heat responses. (*A* and *B*) Confirmation of tissue-specific deletion of Slick in Lbx1-Slick$^{-/-}$ mice. (*A*) Quantitative reverse transcription polymerase chain reaction revealed that in Lbx1-Slick$^{-/-}$ mice, Slick mRNA is selectively reduced in the spinal cord ($t_6 = 32.7$, $P < 0.001$), but remains unaltered in dorsal root ganglia ($t_6 = 0.87$, $P = 0.420$) and the brain cortex ($t_6 = 1.80$, $P = 0.122$; n = 4 per group). Values were normalized to wild-type dorsal root ganglia. (*B*) Immunostaining revealed that Slick immunoreactivity in the superficial dorsal horn is considerably reduced in spinal cords of Lbx1-Slick$^{-/-}$ mice compared with control mice. Weak Slick immunoreactivity was detected throughout the spinal cords of Lbx1-Slick$^{-/-}$ mice, as revealed by comparison with spinal cords of Slick$^{-/-}$ mice. (*C*) Expression of Slack mRNA in Lbx1-Slick$^{-/-}$ and control mice is comparable in dorsal root ganglia ($t_{18} = 1.86$, $P = 0.218$), the spinal cord ($t_{18} = 0.58$, $P = 0.816$), and the brain cortex ($t_{18} = 0.47$, $P = 0.816$; n = 4 per group). (*D* and *E*) Responses to heat stimuli in Lbx1-Slick$^{-/-}$ mice. The behavior of Lbx1-Slick$^{-/-}$ mice was unaltered as compared to control mice in the hot plate test ([*D*] 48°C: $t_{25} = 0.44$, $P = 0.661$; n = 13 [Lbx1-Slick$^{-/-}$], n = 14 [control]; 50°C: $t_{25} = 0.89$, $P = 0.383$; n = 13 [Lbx1-Slick$^{-/-}$], n = 14 [control]; 52°C: $t_{22} = 0.44$, $P = 0.665$; n = 12 per group; 54°C: $t_{22} = 0.80$, $P = 0.431$; n = 12 per group), and in the tail-immersion test ([*E*] 46°C: $t_{30} = 0.37$, $P = 0.714$; 47°C: $t_{30} = 1.85$, $P = 0.075$; 48°C: $t_{30} = 0.05$, $P = 0.957$; 49°C: $t_{30} = 1.00$, $P = 0.323$; n = 16 per group). Data are presented as mean ± SD. *$P < 0.05$. Scale bar = 100 μm (*B*).

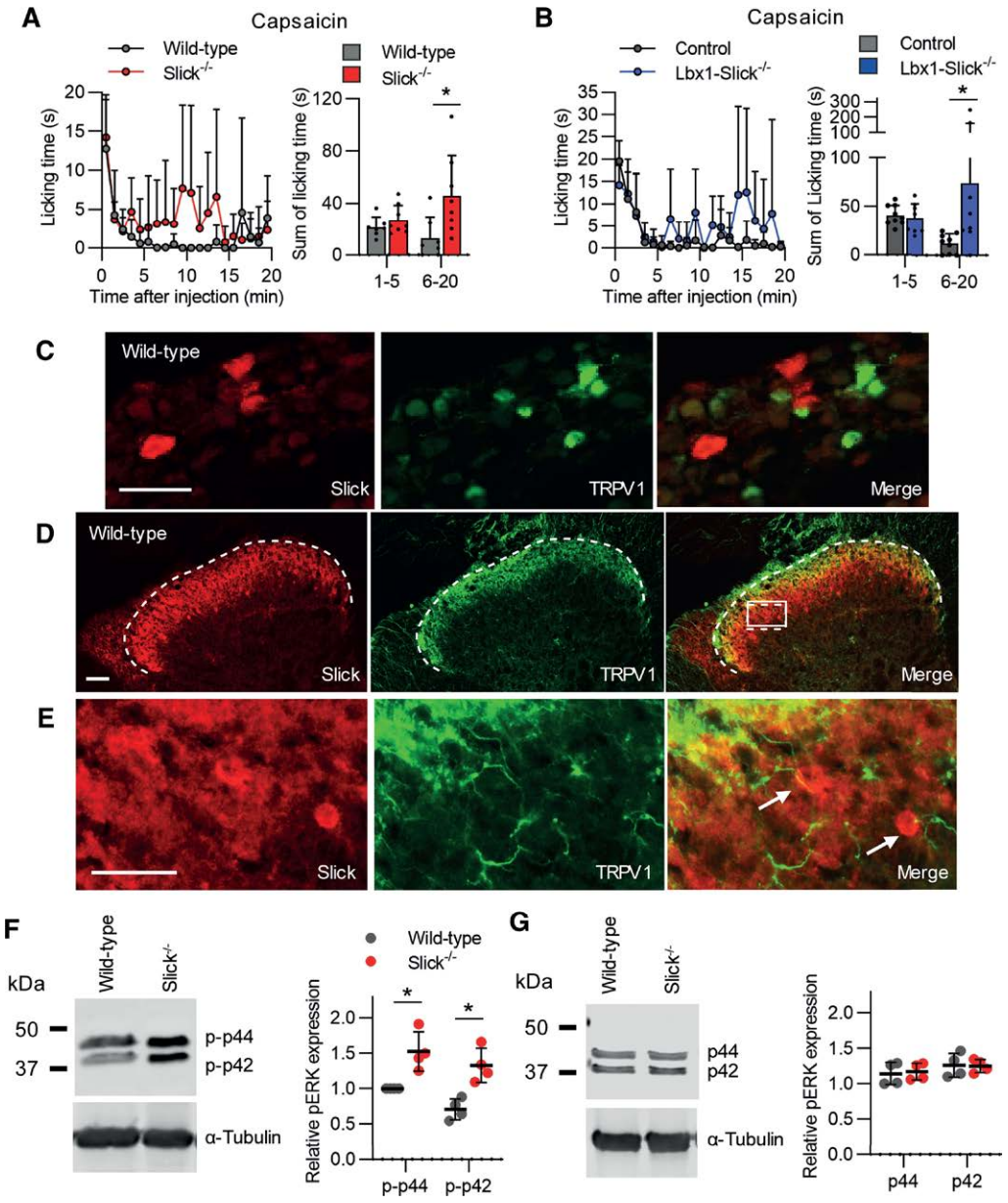

Fig. 6. Increased capsaicin-induced pain behavior in Slick$^{-/-}$ and Lbx1-Slick$^{-/-}$ mice. (*A* and *B*) Capsaicin test in Slick$^{-/-}$ and wild-type mice. *(A)* Capsaicin-induced licking behavior. *(A, left)* Time course of paw licking induced by injection of 5 μg capsaicin into a hind paw. *(A, right)* Sum of paw licking shows that the behavior of Slick$^{-/-}$ mice compared with wild-type mice is normal during the 0- to 5-min period ($t_{26} = 0.57$, $P = 0.574$; n = 8 [Slick$^{-/-}$], n = 7 [wild-type]), but significantly increased during the 6- to 20-min period ($t_{26} = 3.30$, $P = 0.006$; n = 8 [Slick$^{-/-}$], n = 7 [wild-type]) after the capsaicin injection. (*B*) Capsaicin test in Lbx1-Slick$^{-/-}$ and control mice. Similar to Slick$^{-/-}$ mice, Lbx1-Slick$^{-/-}$ mice exhibited an unaltered paw-licking behavior compared with control mice in the first 5 min after capsaicin injection ($t_{30} = 0.16$, $P = 0.871$; n = 8 [Slick$^{-/-}$], n = 9 [wild-type]), whereas the paw licking was significantly increased during the 6- to 20-min period ($t_{30} = 2.97$, $P = 0.012$; n = 8 [Slick$^{-/-}$], n = 9 [wild-type]). (*C*) Double immunostaining of Slick and transient receptor potential vanilloid 1 (TRPV1) in dorsal root ganglia reveals that Slick is virtually absent from TRPV1-positive sensory neurons. (*D*) Double immunostaining of Slick and TRPV1 in the spinal cord shows some overlap of Slick and TRPV1 immunoreactivity. (*E*) Higher magnification of the area marked in the merge picture in *D*. Slick immunoreactivity is in close proximity to the central projections of TRPV1-positive afferent fibers. (*F*) Western blot analysis of phosphorylated extracellular signal–regulated kinase in the spinal cord of wild-type and Slick$^{-/-}$ mice 10 min after capsaicin injection into a hind paw. Data show that phosphorylation of both p44 ($t_{12} = 3.72$, $P = 0.003$; n = 4 per group) and p42 ($t_{12} = 4.39$, $P = 0.002$; n = 4 per group) mitogen-activated protein kinase is significantly increased in Slick$^{-/-}$ mice as compared to wild-type mice. (*G*) Western blot of extracellular signal–regulated kinase in the spinal cord confirmed a similar expression of p44 ($t_{12} = 0.32$, $P = 0.940$; n = 4 per group) and p42 ($t_{12} = 0.10$, $P = 0.940$; n = 4 per group) in Slick$^{-/-}$ and wild-type mice. Values in *F* and *G* were normalized to α-tubulin as loading control and are expressed as relative values compared to phosphorylated p44 expression of wild-type control. Data are presented as mean ± SD. *$P < 0.05$. Scale bars = 50 μm (*C* and *D*); scale bar = 25 μm (*E*).

[n = 8]: 73.6 ± 85.4 s [95% CI, 2.2 to 145.1]; control [n = 9]: 12.3 ± 9.9 s [95% CI, 4.6 to 19.9]; P = 0.012; fig. 6B), but unaltered in the first 5 min as compared with control mice (Lbx1-Slick$^{-/-}$ [n = 8]: 37.5 ± 15.3 s [95% CI, 24.7 to 50.3]; control [n = 9]: 40.9 ± 10.3 s [95% CI, 33.0 to 48.9]; P = 0.871; fig. 6B; results for female and male cohorts are shown in Supplemental Digital Content 3 fig. 3, C and D, http://links.lww.com/ALN/C807). These results indicate that Slick in dorsal horn neurons modulates the pain behavior at a late stage of the capsaicin test.

To further explore this finding, we performed double-labeling immunostaining of Slick and TRPV1 in dorsal root ganglia and the spinal cord. Consistent with the observation that Slick is enriched in Aδ-fibers (fig. 1, F and H) and most TRPV1$^+$ sensory neurons are C-fibers,[28] we found that Slick$^+$ sensory neurons virtually do not coexpress TRPV1 (fig. 6C). In the dorsal horn of the spinal cord, Slick immunoreactivity is partly colocalized with the central projections of TRPV1$^+$ afferent fibers (fig. 6D). Interestingly, at higher magnification, we detected TRPV1$^+$ fibers in close proximity to somata of Slick$^+$ cells (fig. 6E), pointing to a possible interaction of Slick$^+$ dorsal horn neurons and TRPV1$^+$ sensory neurons that respond to capsaicin.

We then performed Western blot analyses of pERK as a marker for neuronal activation in the dorsal horn.[29] Lumbar (L4–L5) spinal cords from wild-type and Slick$^{-/-}$ mice were obtained 10 min after intraplantar capsaicin injection, *i.e.*, at a time point of increased paw licking in Slick$^{-/-}$ mice (compared to fig. 6A). Of note, phosphorylation of ERK1 (p44 MAPK) and ERK2 (p42 MAPK), which both are detected by the anti-pERK antibody, was significantly increased in Slick$^{-/-}$ mice compared with wild-type mice (p-p44, Slick$^{-/-}$: 1.5 ± 0.3 [95% CI, 1.1 to 2.0], wild-type: 1.0 ± 0.0 [95% CI, 1.0 to 1.0], P = 0.003; p-p42, Slick$^{-/-}$: 1.3 ± 0.2 [95% CI, 0.9 to 1.7], wild-type: 0.7 ± 0.1 [95% CI, 0.5 to 0.9]; P = 0.002; n = 4/group; fig. 6F). Control experiments confirmed that ERK1 and ERK2 protein expression is similar between wild-type and Slick$^{-/-}$ mice in the lumbar spinal cord (p44, Slick$^{-/-}$: 1.2 ± 0.1 [95% CI, 1.0 to 1.4], wild-type: 1.1 ± 0.2 [95% CI, 0.9 to 1.4]; P = 0.940; p42, Slick$^{-/-}$: 1.3 ± 0.1 [95% CI, 1.1 to 1.4], wild-type: 1.3 ± 0.2 [95% CI, 1.0 to 1.5]; P = 0.940; n = 4/group; fig. 6G). Together, these data indicate that Slick modulates the activity of dorsal horn neurons in response to TRPV1 activation in sensory neurons.

Slick Is Dispensable for Allyl Isothiocyanate–induced Pain Behavior

In response to peer review, we assessed the behavior after intraplantar injection of the transient receptor potential ankyrin 1 (TRPA1) activator, allyl isothiocyanate, to explore the role of Slick in TRPA1-dependent pain processing. Compared to wild-type mice, Slick$^{-/-}$ mice demonstrated unaltered licking behavior after allyl isothiocyanate injection (Slick$^{-/-}$ [n = 8]: 210.4 ± 127.0 s [95% CI, 104.1 to 316.6]; wild-type [n = 6]: 253.9 ± 166.3 s [95% CI, 79.4 to 428.4]; P = 0.587; fig. 7A). We also tested allyl isothiocyanate–induced mechanical pain sensitivity, but did not observe significant differences between Slick$^{-/-}$ and wild-type mice (baseline: Slick$^{-/-}$ [n = 8]: 0.9 ± 0.1 g [95% CI, 0.8 to 1.0]; wild-type [n = 6]: 0.8 ± 0.1 g [95% CI, 0.7 to 0.9]; P = 0.844; 1 h: Slick$^{-/-}$ [n = 8]: 0.2 ± 0.1 g [95% CI, 0.1 to 0.3]; wild-type [n = 6]: 0.2 ± 0.1 g [95% CI, 0.1 to 0.3]; P > 0.999; 3 h: Slick$^{-/-}$ [n = 8]: 0.2 ± 0.1 g [95% CI, 0.1 to 0.3]; wild-type [n = 6]: 0.2 ± 0.1 g [95% CI, 0.1 to 0.3]; P = 0.935; 5 h: Slick$^{-/-}$ [n = 8]: 0.3 ± 0.2 g [95% CI, 0.2 to 0.4]; wild-type [n = 6]: 0.2 ± 0.1 g [95% CI, 0.1 to 0.2]; P = 0.230; 24 h: Slick$^{-/-}$ [n = 8]: 0.5 ± 0.2 g [95% CI, 0.4 to 0.7]; wild-type: 0.4 ± 0.2 g [95% CI, 0.2 to 0.6]; P = 0.917; fig. 7B). Similar to Slick$^{-/-}$ mice, Lbx1-Slick$^{-/-}$ mice demonstrated intact licking behavior (Lbx1-Slick$^{-/-}$ [n = 7]: 158.3 ± 111.5 s [95% CI, 55.2 to 261.5]; control [n = 8]: 103.0 ± 90.5 s [95% CI, 27.3 to 178.6]; P = 0.308; fig. 7C) and mechanical hypersensitivity (baseline: Lbx1-Slick$^{-/-}$ [n = 5]: 0.9 ± 0.1 g [95% CI, 0.8 to 1.0]; control [n = 6]: 0.9 ± 0.1 g [95% CI, 0.7 to 1.0]; P = 0.995; 1 h: Lbx1-Slick$^{-/-}$ [n = 5]: 0.2 ± 0.1 g [95% CI, 0.1 to 0.3]; control [n = 6]: 0.2 ± 0.1 g [95% CI, 0.1 to 0.3]; P = 0.998; 3 h: Lbx1-Slick$^{-/-}$ [n = 5]: 0.2 ± 0.1 g [95% CI, 0.1 to 0.4]; control [n = 6]: 0.2 ± 0.1 g [95% CI, 0.1 to 0.4]; P > 0.999; 5 h: Lbx1-Slick$^{-/-}$ [n = 5]: 0.3 ± 0.1 g [95% CI, 0.1 to 0.5]; control [n = 6]: 0.2 ± 0.1 g [95% CI, 0.1 to 0.4]; P = 0.986; 24 h: Lbx1-Slick$^{-/-}$ [n = 5]: 0.9 ± 0.2 g [95% CI, 0.6 to 1.2]; control: 0.8 ± 0.2 g [95% CI, 0.6 to 1.0]; P = 0.997; fig. 7D) compared with control mice. Thus, unlike the capsaicin test, Slick seems not to be involved in allyl isothiocyanate–induced pain.

Slick in the Spinal Dorsal Horn Modulates Somatostatin Signaling

To further explore the functional role of Slick in dorsal horn neurons, we focused on the neuropeptide somatostatin, because (1) previous studies reported that somatostatin is released from capsaicin-sensitive sensory nerve terminals in the dorsal horn[30]; (2) immunostaining revealed that SSTR2, the most abundant somatostatin receptor in the spinal cord,[31] is expressed by virtually all GAL$^+$ cells in the dorsal horn[32]—of which approximately 80% are Slick$^+$ (fig. 3D); and (3) single-cell RNA-sequencing data further support a colocalization of SSTR2 and Slick in dorsal horn neuron populations (*i.e.,* both were detected in the Gaba2, 3, 8, and 9 populations of inhibitory interneurons in the dorsal horn).[10] In accordance with these data, we observed a substantial degree of coexpression of Slick mRNA and SSTR2 mRNA in the dorsal horn using double *in situ* hybridization experiments; 50.4 ± 1.6% of Slick$^+$ cells expressed SSTR2, whereas 61.3 ± 7.4% of SSTR2$^+$ cells were positive for Slick (fig. 8A).

We then assessed whether Slick and somatostatin pathways might functionally interact in the dorsal horn. For that purpose, we intrathecally administered the selective SSTR2

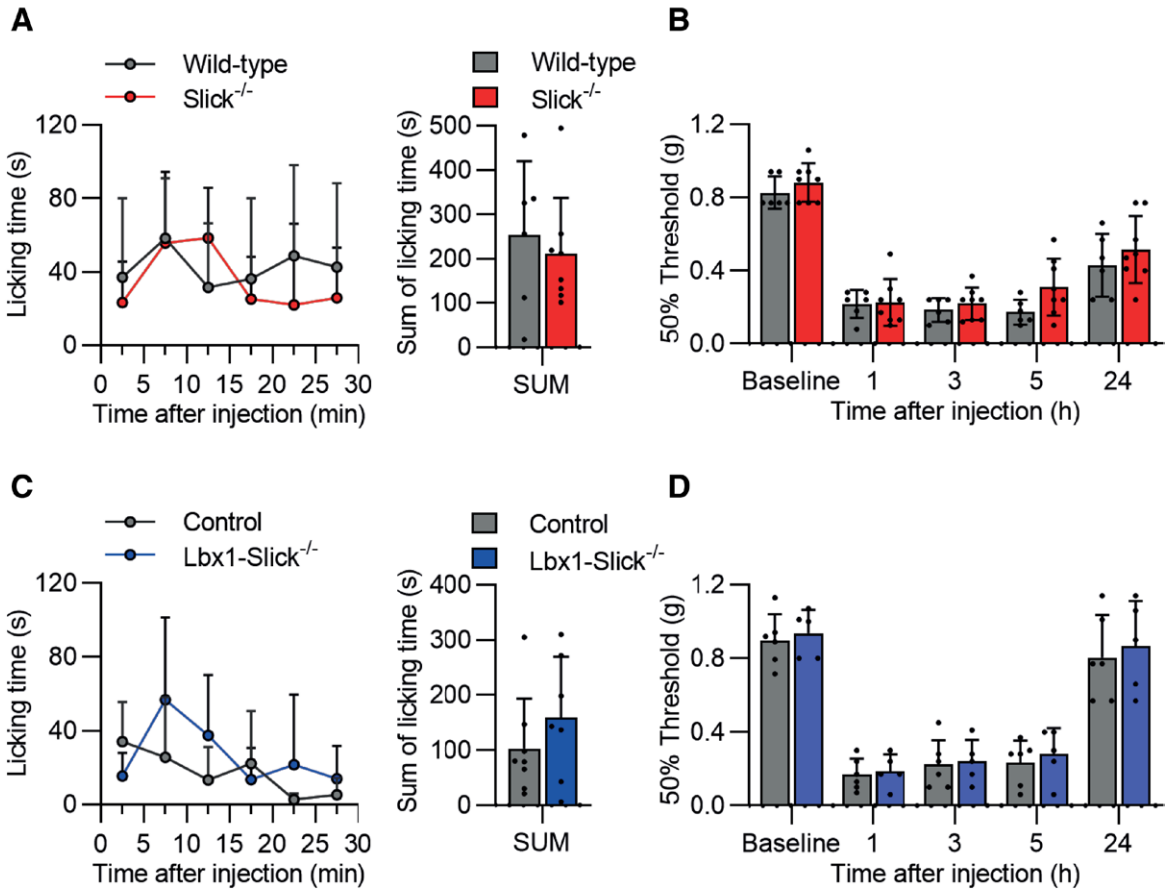

Fig. 7. Allyl isothiocyanate–induced pain behavior in Slick$^{-/-}$ and Lbx1-Slick$^{-/-}$ mice. (*A*) Allyl isothiocyanate test in Slick$^{-/-}$ and wild-type mice. (*A, left*) Time course of paw licking induced by injection of 10 nmol allyl isothiocyanate into a hind paw. (*A, right*) Sum of paw licking shows that the behavior of Slick$^{-/-}$ mice is comparable to wild-type mice during 30 min after the allyl isothiocyanate injection ($t_{12} = 0.56$, $P = 0.587$; n = 8 [Slick$^{-/-}$], n = 6 [wild-type]). (*B*) Intraplantar injection of allyl isothiocyanate elicits similar mechanical hypersensitivity in Slick$^{-/-}$ and wild-type mice ($F[4,48] = 0.91$, $P = 0.464$; n = 8 [Slick$^{-/-}$], n = 6 [wild-type]). (*C*) Allyl isothiocyanate test in Lbx1-Slick$^{-/-}$ and control mice. (*Left*) Time course of paw licking induced by injection of 10 nmol allyl isothiocyanate into a hind paw. (*Right*) Sum of paw licking shows that the behavior of Lbx1-Slick$^{-/-}$ mice is comparable to control mice during 30 min after the allyl isothiocyanate injection ($t_{13} = 1.06$, $P = 0.308$; n = 7 [Lbx1-Slick$^{-/-}$], n = 8 [control]). (*D*) Intraplantar injection of allyl isothiocyanate elicits similar mechanical hypersensitivity in Lbx1-Slick$^{-/-}$ and control mice ($F[4,36] = 0.05$, $P = 0.464$; n = 5 [Lbx1-Slick$^{-/-}$], n = 6 [control]). Data are presented as mean ± SD.

antagonist CYN-154806[18] in Slick$^{-/-}$ and wild-type mice 30 min before intraplantar capsaicin injection and analyzed the pain behavior. Interestingly, the enhanced paw licking in the later phase (6 to 20 min after capsaicin injection; fig. 6A) was absent in Slick$^{-/-}$ mice pretreated with CYN-154806 (Slick$^{-/-}$ [n = 5] *vs.* wild-type [n = 6]: 6.8 ± 4.1 s *vs.* 10.1 ± 12.9 s, respectively; $P = 0.862$; fig. 8B). Similarly, intrathecal CYN-154806 pretreatment prevented the later phase of paw licking in Lbx1-Slick$^{-/-}$ mice (Lbx1-Slick$^{-/-}$ [n = 5] *vs.* control [n = 5]: 16.1 ± 18.9 s *vs.* 19.1 ± 9.9 s, respectively; $P = 0.942$; fig. 8C [compared to fig. 6B]). Together, these data point to a signaling pathway that involves TRPV1^{+} sensory neurons and Slick^{+}/SSTR2^{+} dorsal horn neurons.

Recent studies revealed that somatostatin contributes to the processing of itch in the dorsal horn, and that intrathecal administration of somatostatin or its analog octreotide induces scratching in rodents *via* binding to SSTR2 and subsequent inhibition of inhibitory interneurons.[18,33] We therefore analyzed the scratching behavior of Slick$^{-/-}$ and wild-type mice after intrathecal injection of octreotide. Interestingly, the scratching behavior induced by 100 ng octreotide was observed in wild-type mice but considerably reduced in Slick$^{-/-}$ mice (Slick$^{-/-}$: 6.1 ± 6.7 bouts [95% CI, 0.5 to 11.7]; wild-type: 47.5 ± 51.1 bouts [95% CI, 4.8 to 90.2]; $P = 0.039$, n = 8/group; fig. 8D; results for female and male cohorts are presented in Supplemental Digital Content 4 fig. 4, A and B, http://links.lww.com/ALN/

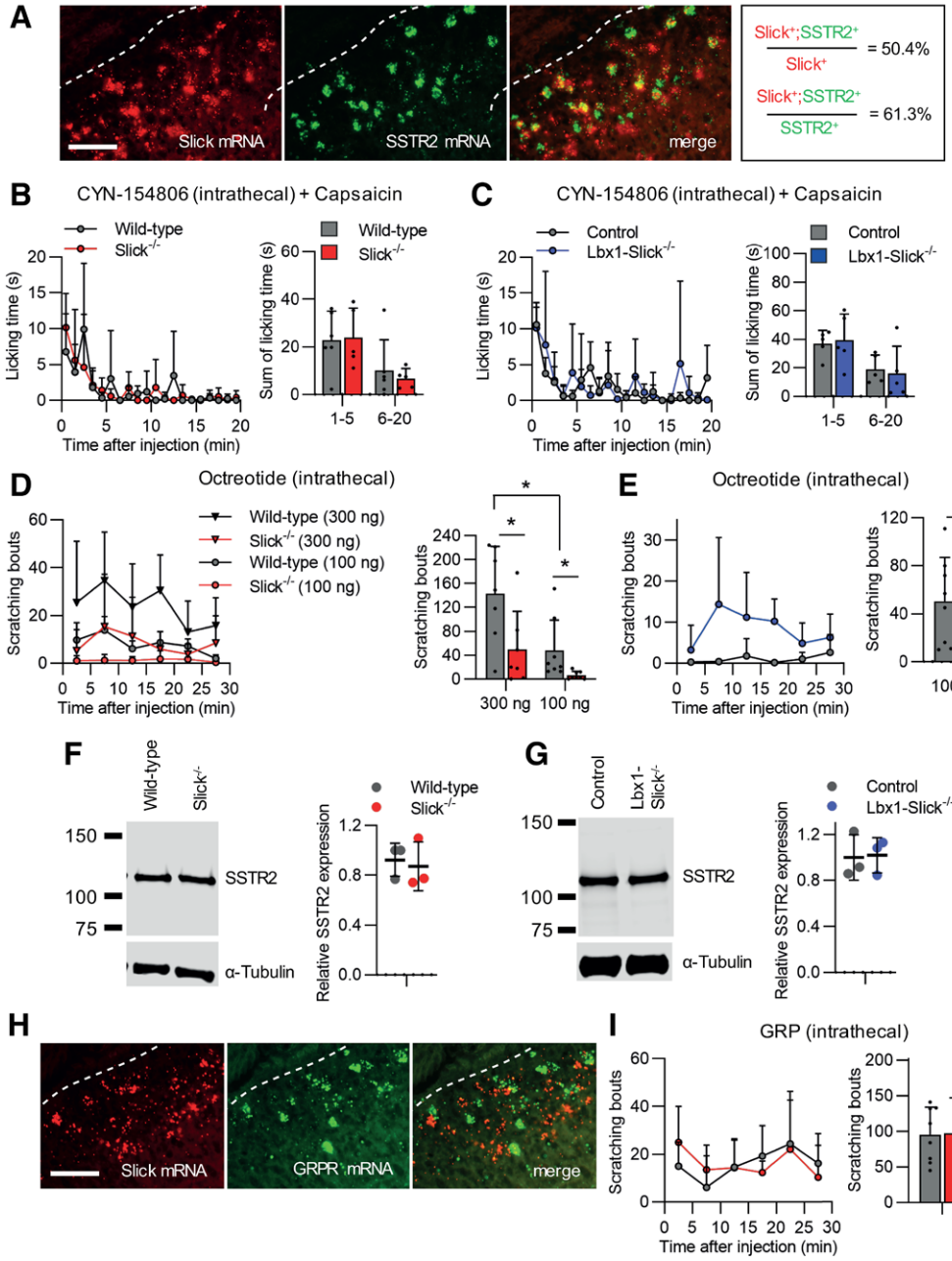

Fig. 8. Slick interacts with somatostatin pathways in pain and itch. (*A*) Double *in situ* hybridization experiments show that Slick and somatostatin receptor 2 (SSTR2) are colocalized in the spinal dorsal horn. (*B* and *C*) Capsaicin test after intrathecal pretreatment with the SSTR2 antagonist CYN-154806 (500 ng in 5 µl NaCl, 0.9%). (*B*) In Slick$^{-/-}$ mice, intrathecal CYN-154806 delivery 30 min before capsaicin injection into a hind paw prevented increased paw licking from 6 to 20 min after capsaicin injection ([compare with fig. 6A] 0 to 5 min: $t_{18} = 0.17$, $P = 0.871$; 5 to 20 min: $t_{18} = 0.50$, $P = 0.862$; n = 5 [Slick$^{-/-}$], n = 6 [wild-type]). (*C*) Similarly, increased paw licking at 6 to 20 min after capsaicin injection (compare with fig. 6B) did not occur in Lbx1-Slick$^{-/-}$ mice pretreated with intrathecal CYN-154806 (0 to 5 min: $t_{16} = 0.26$, $P = 0.942$; 6 to 20 min: $t_{16} = 0.31$, $P = 0.942$; n = 5 per group). (*D* and *E*) Somatostatin-induced itch behavior in Slick$^{-/-}$ and Lbx1-Slick$^{-/-}$ mice. After intrathecal injection of the somatostatin analog octreotide (100 ng and 300 ng in 5 µl NaCl, 0.9%), the scratching behavior during a 30-min period was significantly reduced in Slick$^{-/-}$ mice compared with wild-type mice ([*D*] 100 ng: $t_{14} = 2.27$, $P = 0.039$; n = 8 per group; 300 ng: $t_{12} = 2.43$, $P = 0.032$; n = 7 per group), and in Lbx1-Slick$^{-/-}$ mice compared with control mice ([*E*] $t_{14} = 3.35$, $P = 0.005$; n = 8 per group). (*F* and *G*) Western blot of SSTR2 in the spinal cord from Slick$^{-/-}$ and wild-type mice ([*F*] $t_4 = 0.38$, $P = 0.725$; n = 3 per group) and from Lbx1-Slick$^{-/-}$ and control mice ([*G*] $t_4 = 0.13$, $P = 0.904$; n = 3 per group) demonstrated unaltered SSTR2 expression in the absence of Slick. Values were normalized to α-tubulin as loading control. (*H*) Double *in situ* hybridization of Slick mRNA with gastrin-releasing peptide receptor (GRPR) mRNA in the spinal dorsal horn shows virtually no colocalization. (*I*) After intrathecal injection of gastrin-releasing peptide (GRP), the scratching behavior was unaltered in Slick$^{-/-}$ mice compared to wild-type mice (unpaired two-tailed *t* test: $t_{11} = 0.10$, $P = 0.921$; n = 8 per group). Data are presented as mean ± SD. *$P < 0.05$. Scale bar = 50 µm.

C808). In response to peer review, we also injected 300 ng octreotide to investigate whether the effect is dose-dependent. Indeed, a dose-dependent response to intrathecal octreotide was observed in wild-type mice (100 ng [n = 8]: 47.5 ± 51.1 bouts [95% CI, 4.8 to 90.2]; 300 ng [n = 7]: 142.9 ± 79.1 bouts [95% CI, 69.7 to 216.1]; P = 0.005; fig. 8D), and again, a significant difference in scratching behavior was observed between genotypes (Slick$^{-/-}$ [n = 7]: 49.9 ± 63.4 bouts [95% CI, –8.8 to 108.5]; wild-type [n = 7]: 142.9 ± 79.1 bouts [95% CI, 69.7 to 216.1]; P = 0.032; fig. 8D). Similarly, Lbx1-Slick$^{-/-}$ mice showed a significantly reduced scratching behavior compared with control mice after intrathecal administration of 100 ng octreotide (Lbx1-Slick$^{-/-}$ [n = 8]: 6.1 ± 6.2 bouts [95% CI, 0.9 to 11.3]; control [n = 8]: 50.3 ± 36.8 bouts [95% CI, 19.5 to 81.0]; P = 0.005; fig. 8E; Supplemental Digital Content 4 fig. 4, C and D, http://links.lww.com/ALN/C808). Western blot experiments demonstrated similar SSTR2 levels in the spinal cord and dorsal root ganglia of wild-type and Slick$^{-/-}$ mice (Slick$^{-/-}$ [n = 3] *vs.* wild-type [n =3]: 0.9 ± 0.2 *vs.* 0.9 ± 0.1, respectively; P = 0.725; fig. 7F), and of control and Lbx1-Slick$^{-/-}$ mice (Lbx1-Slick$^{-/-}$ [n = 3] *vs.* control [n = 3]: 1.0 ± 0.2 *vs.* 1.0 ± 0.2, respectively; P = 0.904; fig. 8G), suggesting that there was no compensatory regulation due to the Slick knockout that might have contributed to the observed itch behavior. Together, these data suggest that Slick expressed in dorsal horn neurons is required for the behavioral response to intrathecally administered octreotide.

In control experiments, we intrathecally injected GRP, which evokes scratching *via* activation of its receptor, GRPR, which is almost exclusively expressed in excitatory interneurons.[2,10] Double *in situ* hybridization experiments revealed that GRPR mRNA is virtually absent from Slick^{+} neurons in the dorsal horn (fig. 8H). In line with this observation, the scratching behavior after intrathecal injection of GRP was not significantly altered in Slick$^{-/-}$ mice as compared with wild-type mice (Slick$^{-/-}$ [n = 8] *vs.* wild-type [n = 8]: 97.8 ± 49.5 bouts *vs.* 95.5 ± 38.6 bouts, respectively; P = 0.921; fig. 8I), indicating that the scratching behavior is not generally impaired in Slick knockouts. Altogether, these data suggest that Slick at distinct neuronal populations contributes to pain and itch processing.

Slick Is Not Required for Histamine or Chloroquine-induced Itch

Recent evidence has indicated that Slick$^{-/-}$ mice exhibit normal responses to the pruritic stimuli histamine and chloroquine,[6] but the specific contribution of Slick in the spinal dorsal horn to these pruritic stimuli is unclear. In response to peer review, we analyzed the scratching behavior after intradermal injection of histamine (200 μg) and chloroquine (200 μg) into the nape of the neck. As expected, histamine and chloroquine evoked robust scratching behavior in control mice (fig. 9, A and B). However, similar to Slick$^{-/-}$ and wild-type mice, no differences between Lbx1-Slick$^{-/-}$ mice and control littermates were observed for either histamine (Lbx1-Slick$^{-/-}$ [n = 5] *vs.* control [n = 6]: 59.6 ± 33.6 bouts *vs.* 101 ± 68.7 bouts, respectively; P = 0.249; fig. 9A) or chloroquine (Lbx1-Slick$^{-/-}$ [n = 5] *vs.* control n = 6]): 105.0 ± 28.0 bouts *vs.* 150 ± 88.3 bouts, respectively; P = 0.305; fig. 9B). These results suggest that Slick does not contribute to the processing of histamine- and chloroquine-evoked itch.

Discussion

Using multiple tissue-staining procedures, biochemical assays, and behavioral tests in global and conditional knockout mice, we delineated novel roles of the potassium channel Slick in sensations of both pain and itch. Using immunostaining and *in situ* hybridization, we identified Slick in Aδ-fiber nociceptors and in populations of interneurons in the spinal dorsal horn. Global Slick knockouts demonstrated increased nocifensive responses to noxious heat and intraplantar capsaicin, whereas the scratching behavior induced by intrathecal octreotide was abolished. Our experiments in tissue-specific Lbx1-Slick$^{-/-}$ mice revealed that Slick localized to dorsal horn neurons modulates capsaicin and octreotide behavior, but not noxious heat responses. In combination with previous reports,[6,7] the fact that in our study both Slick$^{-/-}$ and Lbx1-Slick$^{-/-}$ mice displayed normal responses to cold and mechanical stimuli, as well as after intrathecal GRP injection supports the hypothesis that Slick exerts distinct functions in pain and itch pathways.

Slick$^{-/-}$ mice showed enhanced sensitivity to heat stimuli at 48° to 50°C in the hot plate test and at 46° to 48°C in the tail-immersion test, but had normal responses after exposure to higher temperatures. This implies that Slick, which may inhibit pain processing in sensory neurons by potassium efflux across the plasma membrane, modulates heat pain only in a certain temperature range. During the past 2 decades, several ion channels have been identified as potential molecular thermosensors in mammals. These include various temperature-sensitive members of the TRP channel family (*e.g.,* TRPV1, TRPV2, TRPV3, TRPV4, TRPA1, TRPM2, TRPM3, and TRPM8); the Ca^{2+}-activated chloride channel, anoctamin 1; stromal interaction molecule 1 (STIM1); members of the two-pore domain potassium channel family (such as KCNK2, KCNK4, and KCNK10); and Nav1.8 channels.[34] Many studies illustrate that these channels are sensitive to heat or cold at different temperature ranges. This is also reflected by the phenotypic profile of respective knockout mice in pain models. For example, TRPV1$^{-/-}$ mice showed impaired behavioral responses in the hot plate test at temperatures greater than or equal to 52.5°C, as well as in the tail-immersion test at temperatures of 50°C, but showed normal responses at lower temperatures.[28] Furthermore, TRPM3$^{-/-}$ mice exhibited increased hot plate latencies at temperatures 52°C or

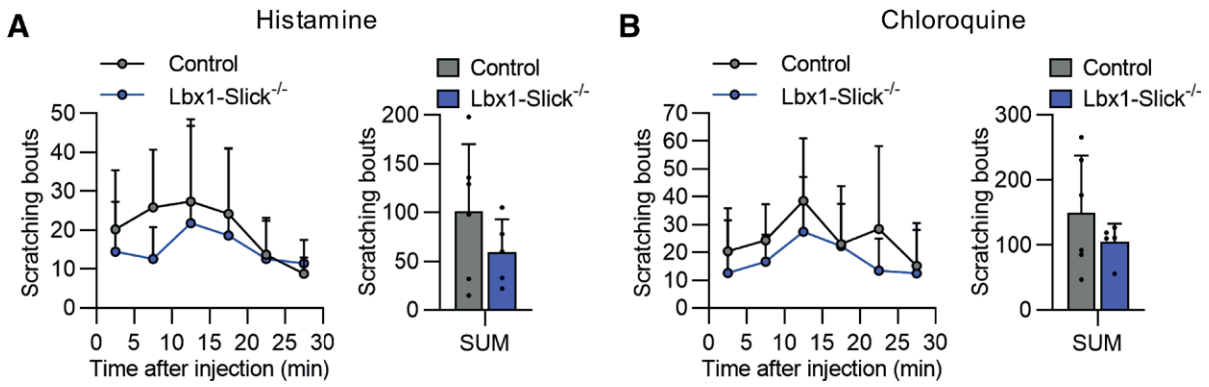

Fig. 9. Lbx1-Slick$^{-/-}$ mice show normal itch behavior after injection of histamine or chloroquine. (*A*) Histamine-induced scratching behavior in Lbx1-Slick$^{-/-}$ and control mice. (*A, left*) Time course of scratching bouts induced by injection of 200 µg histamine into the nape of the neck. (*A, right*) Total scratching bouts within 30 min after histamine injection. Note that histamine-induced itch behavior is comparable between Lbx1-Slick$^{-/-}$ and control mice (unpaired two-tailed *t* test: $t_9 = 1.23$, $P = 0.249$; n = 5 [Lbx1-Slick$^{-/-}$], n = 6 [control]). (*B*) Chloroquine-induced itch behavior in Lbx1-Slick$^{-/-}$ and control mice. (*B, left*) Time course of scratching bouts induced *via* 200 µg chloroquine injection into nape of the neck. (*B, right*) Total scratching bouts within 30 min after chloroquine injection (unpaired two-tailed *t* test: $t_9 = 1.09$, $P = 0.305$; n = 5 [Lbx1-Slick$^{-/-}$], n = 6 [control]). Data are presented as mean ± SD.

higher and unaltered latencies at 50°C, whereas their latencies in the tail immersion test were increased in the range of 45° to 57°C.[35] Conversely, TRPM2$^{-/-}$ mice showed a deficit in their sensation of non-noxious warm temperatures.[36] While TRPA1$^{-/-}$ mice demonstrated a normal behavior on a 50 to 55°C hot plate,[37] a recent study revealed that triple knockouts lacking TRPA1, TRPV1 and TRPM3 show considerably reduced responses to noxious heat at 45° to 52°C in the hot plate test and at 45° to 57°C in the tail-flick test,[13,38] implicating that noxious heat sensing in a wide temperature spectrum essentially relies on these three TRP channels. Future work will be necessary to determine the mechanism underlying the specific modulation of heat sensation by Slick.

In addition to its function in acute heat pain, our study provides several lines of evidence that Slick expressed in the spinal cord contributes to nociceptive signaling between TRPV1$^+$ sensory neurons and SSTR2$^+$ dorsal horn neurons. First, both Slick$^{-/-}$ and Lbx1-Slick$^{-/-}$ mice showed a prolonged paw licking behavior after intraplantar injection of the TRPV1 activator capsaicin. The altered behavior in Lbx1-Slick$^{-/-}$ mice suggests that this phenotype is driven by Slick in dorsal horn neurons. Second, the prolonged capsaicin paw licking was paralleled by increased phosphorylation of the neuronal activity marker ERK in spinal cord extracts of Slick$^{-/-}$ mice. Third, the prolonged capsaicin paw licking in Slick$^{-/-}$ and Lbx1-Slick$^{-/-}$ mice was abolished by intrathecal pretreatment with the SSTR2 antagonist CYN-154806. This finding is in accordance with previous reports that the activation of TRPV1$^+$ sensory neurons—which largely project to lamina I and outer lamina II in the spinal cord[39]—results not only in glutamate release from presynaptic terminals[40] but also in the release of neuropeptides, including somatostatin.[41] In general, somatostatin exerts a wide range of effects that are mediated *via* SSTR1-5 (somatostatin cell-surface receptor subtypes 1 through 5), which belong to the seven transmembrane G protein–coupled receptor superfamily.[42] Among these, SSTR2 is dominantly detected in the dorsal horn of the spinal cord,[10,43] and several studies implicate important functions of SSTR2 in the processing of pain and itch.[18,33] Like all other SST receptors, SSTR2 associates with the pertussis toxin–sensitive Gi protein and is coupled to adenylate cyclase and other signaling pathways,[42] and SSTR2 activation has been shown to result in membrane hyperpolarization and inhibition of exocytosis.[42,44] Our finding that intrathecal CYN-154806 abolished the prolonged capsaicin-induced licking behavior in Slick$^{-/-}$ and Lbx1-Slick$^{-/-}$ mice, but did not affect the behavior in control mice, points to an increased activity of SSTR2$^+$ dorsal horn neurons in the absence of Slick. Considering that SSTR2$^+$ dorsal horn neurons mostly release GABA,[10] one might assume that after capsaicin injection, somatostatin inhibits the GABA release from SSTR2$^+$ dorsal horn neurons in a Slick-dependent manner. Further studies are needed to elucidate the mechanisms by which Slick$^+$/SSTR2$^+$ dorsal horn neurons limit the nocifensive response to intraplantar capsaicin. It must also be considered that the response of an interneuronal population to a given sensory modality is defined not only by its peripheral afferent input but also by the neuronal input it receives from other local circuit interneurons.[45]

A function of Slick in SSTR2$^+$ dorsal horn neurons is further supported by the considerably reduced scratching

behavior of Slick$^{-/-}$ and Lbx1-Slick$^{-/-}$ mice after intrathecal injection of octreotide, which binds preferentially to SSTR2 with only moderate affinity for SSTR5 and SSTR3.[42] Given the prolonged nocifensive behavior of Slick-deficient mice after intraplantar capsaicin, their ameliorated itch behavior was quite surprising. However, these apparently contrasting functions of Slick in pain and itch are in line with the complex interactions between the circuitries for pain and itch within the dorsal horn that were reported in previous studies (for review, see Lay and Dong,[2] Koch *et al.*,[45] and Chen and Sun[46]). The essential function of SSTR2$^+$ interneurons in both pain and itch has been demonstrated in several previous studies. For example, Huang *et al.* demonstrated that intrathecal octreotide potentiates itch through disinhibition of SSTR2$^+$ inhibitory interneurons, which results in disinhibition of GRPR$^+$ neurons that exert a key function in the processing of itch.[18] Moreover, many SSTR2$^+$ dorsal horn neurons contain the transcription factor helix-loop-helix family member B5 (Bhlhb5).[44] The essential function of Bhlhb5$^+$ interneurons in itch processing is reflected by the observation that mice lacking Bhlhb5 develop self-inflicted skin lesions and elevated scratching in response to various pruritogens.[47] As the deletion of Bhlhb5 resulted in a substantial loss of spinal interneurons expressing GAL and nNOS, while other inhibitory neuronal populations expressing NPY or PVALB remained intact, it was concluded that spinal GAL$^+$ and nNOS$^+$ interneurons both can play a key role in gating chemical itch.[47] Therefore, the enrichment of Slick in spinal interneurons expressing GAL, nNOS (fig. 3, D and E), and SSTR2 (fig. 8A) further supports a function of Slick in itch pathways. Furthermore, Bhlhb5$^+$ interneurons are thought to suppress itch *via* cross-activation by nociceptive afferents (including those responding to capsaicin), such that the priming of Bhlhb5$^+$ interneurons by a nociceptive stimulus inhibits itch transmission.[45,48] These findings are in accordance with the contrasting pain and itch behavior of Slick-deficient mice we report in our study. Similar contrasting phenotypes have also been observed in other knockout strains, such as mice lacking somatostatin[18] or VGLUT2.[49] Future studies are needed to further elucidate the circuits of pain and itch, and the mechanisms by which they interact.

In conclusion, we here provide evidence that Slick in distinct populations of sensory neurons and dorsal horn neurons exerts specific functions in the processing of pain and itch.

Acknowledgments

The authors thank Carmen Birchmeier, Ph.D., (Max Delbrueck Center for Molecular Medicine, Berlin, Germany) for providing Lbx1-Cre mice and Sylvia Oßwald, Cyntia Schäfer, R.Ph., and Uli Hermanni (Institute of Pharmacology and Clinical Pharmacy, Goethe University Frankfurt, Frankfurt am Main, Germany) for their excellent technical assistance.

Research Support

This work was supported by the Else Kröner-Fresenius-Stiftung (2015_A98; to Dr. Lu), and the German Research Foundation (LU 2514/1-1; to Dr. Lu, and FOR 2060 project SCHM 2629/3-1; to Dr. Schmidtko).

Competing Interests

Dr. Lukowski received research support from Cyclerion (Cambridge, Massachusetts). Dr. Schmidtko has acted as a consultant in the last 2 yr for Merz Pharma (Frankfurt, Germany) and STADA (Bad Vilbel, Germany). The other authors declare no competing interests.

Correspondence

Address correspondence to Dr. Lu: Institute of Pharmacology and Clinical Pharmacy, Goethe University Frankfurt, Max-von-Laue-Str. 9, 60438 Frankfurt am Main, Germany. lu@em.uni-frankfurt.de.

References

1. Dubin AE, Patapoutian A: Nociceptors: The sensors of the pain pathway. J Clin Invest 2010; 120:3760–72
2. Lay M, Dong X: Neural mechanisms of itch. Annu Rev Neurosci 2020; 43:187–205
3. Waxman SG, Zamponi GW: Regulating excitability of peripheral afferents: Emerging ion channel targets. Nat Neurosci 2014; 17:153–63
4. Tsantoulas C, McMahon SB: Opening paths to novel analgesics: The role of potassium channels in chronic pain. Trends Neurosci 2014; 37:146–58
5. Lu R, Bausch AE, Kallenborn-Gerhardt W, Stoetzer C, Debruin N, Ruth P, Geisslinger G, Leffler A, Lukowski R, Schmidtko A: Slack channels expressed in sensory neurons control neuropathic pain in mice. J Neurosci 2015; 35:1125–35
6. Martinez-Espinosa PL, Wu J, Yang C, Gonzalez-Perez V, Zhou H, Liang H, Xia XM, Lingle CJ: Knockout of Slo2.2 enhances itch, abolishes KNa current, and increases action potential firing frequency in DRG neurons. Elife 2015; 4:e10013
7. Tomasello DL, Hurley E, Wrabetz L, Bhattacharjee A: Slick (Kcnt2) sodium-activated potassium channels limit peptidergic nociceptor excitability and hyperalgesia. J Exp Neurosci 2017; 11:1179069517726996
8. Kaczmarek LK: Slack, slick and sodium-activated potassium channels. ISRN Neurosci 2013; 2013:354262
9. Ferreira JJ, Butler A, Stewart R, Gonzalez-Cota AL, Lybaert P, Amazu C, Reinl EL, Wakle-Prabagaran M,

Salkoff L, England SK, Santi CM: Oxytocin can regulate myometrial smooth muscle excitability by inhibiting the Na+ -activated K+ channel, Slo2.1. J Physiol 2019; 597:137–49
10. Häring M, Zeisel A, Hochgerner H, Rinwa P, Jakobsson JET, Lönnerberg P, La Manno G, Sharma N, Borgius L, Kiehn O, Lagerström MC, Linnarsson S, Ernfors P: Neuronal atlas of the dorsal horn defines its architecture and links sensory input to transcriptional cell types. Nat Neurosci 2018; 21:869–80
11. Schwenk F, Baron U, Rajewsky K: A cre-transgenic mouse strain for the ubiquitous deletion of loxP-flanked gene segments including deletion in germ cells. Nucleic Acids Res 1995; 23:5080–1
12. Sieber MA, Storm R, Martinez-de-la-Torre M, Müller T, Wende H, Reuter K, Vasyutina E, Birchmeier C: Lbx1 acts as a selector gene in the fate determination of somatosensory and viscerosensory relay neurons in the hindbrain. J Neurosci 2007; 27:4902–9
13. Vandewauw I, De Clercq K, Mulier M, Held K, Pinto S, Van Ranst N, Segal A, Voet T, Vennekens R, Zimmermann K, Vriens J, Voets T: A TRP channel trio mediates acute noxious heat sensing. Nature 2018; 555:662–6
14. Luiz AP, MacDonald DI, Santana-Varela S, Millet Q, Sikandar S, Wood JN, Emery EC: Cold sensing by NaV1.8-positive and NaV1.8-negative sensory neurons. Proc Natl Acad Sci U S A 2019; 116:3811–6
15. Brenner DS, Golden JP, Gereau RW IV: A novel behavioral assay for measuring cold sensation in mice. PLoS One 2012; 7:e39765
16. Ranade SS, Woo SH, Dubin AE, Moshourab RA, Wetzel C, Petrus M, Mathur J, Bégay V, Coste B, Mainquist J, Wilson AJ, Francisco AG, Reddy K, Qiu Z, Wood JN, Lewin GR, Patapoutian A: Piezo2 is the major transducer of mechanical forces for touch sensation in mice. Nature 2014; 516:121–5
17. Lu R, Flauaus C, Kennel L, Petersen J, Drees O, Kallenborn-Gerhardt W, Ruth P, Lukowski R, Schmidtko A: KCa3.1 channels modulate the processing of noxious chemical stimuli in mice. Neuropharmacology 2017; 125:386–95
18. Huang J, Polgár E, Solinski HJ, Mishra SK, Tseng PY, Iwagaki N, Boyle KA, Dickie AC, Kriegbaum MC, Wildner H, Zeilhofer HU, Watanabe M, Riddell JS, Todd AJ, Hoon MA: Circuit dissection of the role of somatostatin in itch and pain. Nat Neurosci 2018; 21:707–16
19. Chen H, Kronengold J, Yan Y, Gazula VR, Brown MR, Ma L, Ferreira G, Yang Y, Bhattacharjee A, Sigworth FJ, Salkoff L, Kaczmarek LK: The N-terminal domain of Slack determines the formation and trafficking of Slick/Slack heteromeric sodium-activated potassium channels. J Neurosci 2009; 29:5654–65
20. Castañeda-Corral G, Jimenez-Andrade JM, Bloom AP, Taylor RN, Mantyh WG, Kaczmarska MJ, Ghilardi JR, Mantyh PW: The majority of myelinated and unmyelinated sensory nerve fibers that innervate bone express the tropomyosin receptor kinase A. Neuroscience 2011; 178:196–207
21. Albisetti GW, Ghanem A, Foster E, Conzelmann KK, Zeilhofer HU, Wildner H: Identification of two classes of somatosensory neurons that display resistance to retrograde infection by rabies virus. J Neurosci 2017; 37:10358–71
22. The Oxford Handbook of the Neurobiology of Pain. Edited by Wood JN. New York, Oxford University Press, 2020
23. Usoskin D, Furlan A, Islam S, Abdo H, Lönnerberg P, Lou D, Hjerling-Leffler J, Haeggström J, Kharchenko O, Kharchenko PV, Linnarsson S, Ernfors P: Unbiased classification of sensory neuron types by large-scale single-cell RNA sequencing. Nat Neurosci 2015; 18:145–53
24. Tejada MA, Hashem N, Calloe K, Klaerke DA: Heteromeric Slick/Slack K+ channels show graded sensitivity to cell volume changes. PLoS One 2017; 12:e0169914
25. Hughes DI, Todd AJ: Central nervous system targets: Inhibitory interneurons in the spinal cord. Neurotherapeutics 2020; 17:874–85
26. Peirs C, Williams SP, Zhao X, Walsh CE, Gedeon JY, Cagle NE, Goldring AC, Hioki H, Liu Z, Marell PS, Seal RP: Dorsal horn circuits for persistent mechanical pain. Neuron 2015; 87:797–812
27. Smith KM, Browne TJ, Davis OC, Coyle A, Boyle KA, Watanabe M, Dickinson SA, Iredale JA, Gradwell MA, Jobling P, Callister RJ, Dayas CV, Hughes DI, Graham BA: Calretinin positive neurons form an excitatory amplifier network in the spinal cord dorsal horn. Elife 2019; 8:e49190
28. Caterina MJ, Leffler A, Malmberg AB, Martin WJ, Trafton J, Petersen-Zeitz KR, Koltzenburg M, Basbaum AI, Julius D: Impaired nociception and pain sensation in mice lacking the capsaicin receptor. Science 2000; 288:306–13
29. Gao YJ, Ji RR: c-Fos and pERK, which is a better marker for neuronal activation and central sensitization after noxious stimulation and tissue injury? Open Pain J 2009; 2:11–7
30. Helyes Z, Szabó A, Németh J, Jakab B, Pintér E, Bánvölgyi A, Kereskai L, Kéri G, Szolcsányi J: Antiinflammatory and analgesic effects of somatostatin released from capsaicin-sensitive sensory nerve terminals in a Freund's adjuvant-induced chronic arthritis model in the rat. Arthritis Rheum 2004; 50:1677–85
31. Günther T, Tulipano G, Dournaud P, Bousquet C, Csaba Z, Kreienkamp HJ, Lupp A, Korbonits M, Castaño JP, Wester HJ, Culler M, Melmed S, Schulz S: International Union of Basic and Clinical Pharmacology. CV.

Somatostatin receptors: Structure, function, ligands, and new nomenclature. Pharmacol Rev 2018; 70:763–835
32. Polgár E, Durrieux C, Hughes DI, Todd AJ: A quantitative study of inhibitory interneurons in laminae I-III of the mouse spinal dorsal horn. PLoS One 2013; 8:e78309
33. Fatima M, Ren X, Pan H, Slade HFE, Asmar AJ, Xiong CM, Shi A, Xiong AE, Wang L, Duan B: Spinal somatostatin-positive interneurons transmit chemical itch. Pain 2019; 160:1166–74
34. Vriens J, Nilius B, Voets T: Peripheral thermosensation in mammals. Nat Rev Neurosci 2014; 15:573–89
35. Vriens J, Owsianik G, Hofmann T, Philipp SE, Stab J, Chen X, Benoit M, Xue F, Janssens A, Kerselaers S, Oberwinkler J, Vennekens R, Gudermann T, Nilius B, Voets T: TRPM3 is a nociceptor channel involved in the detection of noxious heat. Neuron 2011; 70:482–94
36. Tan CH, McNaughton PA: The TRPM2 ion channel is required for sensitivity to warmth. Nature 2016; 536:460–3
37. Kwan KY, Allchorne AJ, Vollrath MA, Christensen AP, Zhang DS, Woolf CJ, Corey DP: TRPA1 contributes to cold, mechanical, and chemical nociception but is not essential for hair-cell transduction. Neuron 2006; 50:277–89
38. Vilar B, Tan CH, McNaughton PA: Heat detection by the TRPM2 ion channel. Nature 2020; 584:E5–E12
39. Basbaum AI, Bautista DM, Scherrer G, Julius D: Cellular and molecular mechanisms of pain. Cell 2009; 139:267–84
40. Park CK, Lü N, Xu ZZ, Liu T, Serhan CN, Ji RR: Resolving TRPV1- and TNF-α-mediated spinal cord synaptic plasticity and inflammatory pain with neuroprotectin D1. J Neurosci 2011; 31:15072–85
41. Szolcsányi J, Helyes Z, Oroszi G, Németh J, Pintér E: Release of somatostatin and its role in the mediation of the anti-inflammatory effect induced by antidromic stimulation of sensory fibres of rat sciatic nerve. Br J Pharmacol 1998; 123:936–42
42. Theodoropoulou M, Stalla GK: Somatostatin receptors: From signaling to clinical practice. Front Neuroendocrinol 2013; 34:228–52
43. Bowman BR, Bokiniec P, McMullan S, Goodchild AK, Burke PGR: Somatostatin 2 receptors in the spinal cord tonically restrain thermogenic, cardiac and other sympathetic outflows. Front Neurosci 2019; 13:121
44. Kardon AP, Polgár E, Hachisuka J, Snyder LM, Cameron D, Savage S, Cai X, Karnup S, Fan CR, Hemenway GM, Bernard CS, Schwartz ES, Nagase H, Schwarzer C, Watanabe M, Furuta T, Kaneko T, Koerber HR, Todd AJ, Ross SE: Dynorphin acts as a neuromodulator to inhibit itch in the dorsal horn of the spinal cord. Neuron 2014; 82:573–86
45. Koch SC, Acton D, Goulding M: Spinal circuits for touch, pain, and itch. Annu Rev Physiol 2018; 80:189–217
46. Chen XJ, Sun YG: Central circuit mechanisms of itch. Nat Commun 2020; 11:3052
47. Ross SE, Mardinly AR, McCord AE, Zurawski J, Cohen S, Jung C, Hu L, Mok SI, Shah A, Savner EM, Tolias C, Corfas R, Chen S, Inquimbert P, Xu Y, McInnes RR, Rice FL, Corfas G, Ma Q, Woolf CJ, Greenberg ME: Loss of inhibitory interneurons in the dorsal spinal cord and elevated itch in Bhlhb5 mutant mice. Neuron 2010; 65:886–98
48. Hachisuka J, Baumbauer KM, Omori Y, Snyder LM, Koerber HR, Ross SE: Semi-intact *ex vivo* approach to investigate spinal somatosensory circuits. Elife 2016; 5:e22866
49. Liu Y, Abdel Samad O, Zhang L, Duan B, Tong Q, Lopes C, Ji RR, Lowell BB, Ma Q: VGLUT2-dependent glutamate release from nociceptors is required to sense pain and suppress itch. Neuron 2010; 68:543–56